Seminar series nr 133

Investigating the Impact of Ground Reflectance on Satellite Estimates of Forest Leaf Area Index

Per Persson

2007
Geobiosphere Science Centre
Physical Geography and Ecosystems Analysis
Lund University
Sölvegatan 12
S-223 62 Lund
Sweden

Investigating the Impact of Ground Reflectance on Satellite Estimates of Forest Leaf Area Index

By: Per Persson, 2007

Supervisor:
Ph.D. Lars Eklundh,
Institution of Physical Geography and Ecosystem Analysis,
Lund University

A Master Degree-thesis in Physical Geography and Ecosystem Analysis,
Geobiosphere Science Centre,
Institution of Physical Geography and Ecosystem Analysis,
Lund University,
Sweden

Acknowledgement

I first whish to thank my co-worker Emma Persson for all help from field campaign to modeling events, this vast amount of data would not have been possible to collect and analyze without you. I thank my supervisor PhD Lars Eklundh for satellite data, ideas and new angles to problems arising but most of all for being a great supporter throughout the process, and Helena Eriksson for critical thoughts during the writing process and valuable knowledge and help during data analysis. I also whish to thank Andres Kuusk at Tartu Observatory Estonia for help with the inversion modeling. At last I whish to thank my father Rune Persson, my mother Ingrid Andersson and Maria Munch for their support throughout the work and for believing in me all the way.

Abstract

Ground reflectance of forests has been suggested as a main source weakening the strength of relationships using satellite reflectance to predict forest leaf area index (LAI), a key input variable in models of carbon balance and global circulation. In this project a radiative transfer model was used to simulate the influence of ground reflectance in forest canopy reflectance in twenty forest stands in Scania (Southern Sweden). Data needed to run the model were retrieved from measurements in the stands (14 deciduous and 6 coniferous) that were of varying tree density, canopy structure and ground cover. The variation in forest reflectance due to the influence of ground reflectance was found to be significantly negatively related to forest reflectance for the coniferous stands. However, no such relationship was found for the deciduous stands. When the influence on LAI predicted from satellite reflectance was estimated it was found that the variation in ground reflectance had a huge impact on predicted LAI, especially for lower LAI. Significant negative relationships were also found between canopy LAI estimates and modelled LAI of the ground vegetation for all the forest stands (r^2=0.49). The relationships were stronger when deciduous and coniferous stands were separated. The results point towards that ground reflectance has a major impact on forest canopy reflectance, and seriously decreases the accuracy of LAI predicted by empirical relationships of satellite reflectance. Correction of the satellite reflectance for ground reflectance is suggested in order to achieve more reliable LAI estimates for sub-boreal forests.

Sammanfattning

Bladyteindex för skog är ett mått på mängden blad i skogen. Bladyteindexet används i klimatmodeller för att uppskatta viktiga biologiska processer för skogen som fotosyntes, evapotranspiration och kolutbyte med atmosfären. Dessa modeller behöver bladyteindexdata över stora skogsarealer, som rimligtvis inte kan mätas för hand. Man har upptäckt samband mellan satellitdata i form av skogars reflektans (andel reflekterat ljus per andel infallande ljus) enligt vissa våglängdskombinationer (vegetationsindex) och bladyteindex uppmätt från marken. Dessa samband kan användas till att beräkna bladyteindex från satellitdata vilket skulle tillfredställa behovet av bladyteindexdata över stora skogsarealer. Sambanden är troligtvis inte tillräckligt starka till följd av diverse felkällor och skulle kunna ge missvisande värden på bladyteindex om de användes. En möjligtvis stor felkälla antas vara det reflekterade ljuset från marken i skogen (markreflektans). Markreflktansen läggs till reflektansen från trädkronorna och verkar på så vis som en störande faktor i sambanden mellan vegetationsindex och bladyteindex. Denna studie har som mål att uppskatta värden på markreflektans för lövskog och barrskog, samt att uppskatta markreflektansens påverkan på bladyteindex beräknat från samband mellan olika vegetationsindex och bladyteindex uppmätt i skogen. För att göra detta använde jag mig av en matematisk modell av skogen som simulerar dess reflektans och uppmätta parametrar till modellen från 14 lövskogs- och 6 barrskogsbestånd i Skåne. I modellen finns en delmodell som simulerar markreflektans. Genom att i modellen variera markreflektansens inverkan på skogens reflektans utifrån dess naturliga variation uppmätt i skogen kunde skillnaden i skogens totala reflektans till följd av variationen i markreflektans beräknas. Jag fann två negativa statistiskt säkerställda samband mellan markreflektans och vetetationsindex vilka indikerar att andelen markreflektans i ett vegetationsindex ökar ju mindre vegetation som finns i trädkronorna. Detta innebär att markreflektans gör bladyteindexvärden som beräknas utifrån sambanden osäkra, och att osäkerheten ökar ju lägre värdet på bladyteindex är. Således är markreflektansens påverkan på bladyteindex uppskattat från satellitdata stor. Man bör därför vara försiktig när man använder bladyteindex framtaget på detta sätt i klimatmodellerna. För att kunna använda satellitdata till att beräkna bladyteindex föreslås vidare att satellitdatan korrigeras för markreflektansens påverkan och att dessa korrigerade satellitdata används till att upprätta nya samband till bladyteindex för skog som förhoppningsvis är starkare.

Dictionary

ARVI: Atmospheric reduction vegetation index. See also SVI.

BAI: Branch area index. Defined as one half the total surface area of branches per unit ground surface area.

cAB : leaf chlorophyll concentration (microgr./m^2 leaf area), a PROSPECT parameter

CR: Canopy reflectance.

EWT : equivalent water thickness (cm ≈ g/m^2), a measure of leaf water content, a PROSPECT parameter

FRT: Forest reflectance transmittance. A forest radiative transfer model, simulating forest reflectance in 400-2500nm, made by Tiit Nilson, and Andres Kuusk at Tartu Observatory, Estonia.

GCM: Global Circulation Model.

LAI: A measure of the amount of leaf area. Defined as half the total leaf area per unit ground area (Chen and Black, 1992).

LAI 2000: see PCA

L_{Chen}: A LAI estimate calculated as; $L_{Chen} = L_e (1 - \alpha) \gamma / \Omega$

L_e: Effective LAI measured by the PCA.

L_{Gower}: A LAI estimate calculated as; $L_{Gower} = L_e * \gamma$

MCRM(2): Model for ground reflectance used in FRT made by Andres Kuusk at Tartu Observatory, Estonia. Also for separate use.

NDVI: Normalised difference vegetation index. See also SVI.

NIR: near infrared radiation

PCA: plant canopy analyzer; A optical handheld instrument used for estimation of LAI.

PROSPECT: Model for leaf reflectance used in FRT. See (Jacquemoud and Barret, 1990; Jacquemoud *et al*., 1996). Also for separate use.

red edge: The steep increase in reflectance in the red part (close to <700nm) of a typical vegetation spectrum.

SAVI: Soil adjusted vegetation index. See also SVI.

SLW : Specific Leaf Weight (g/m^2), a PROSPECT parameter

SR: Simple Ratio. A vegetation index. Also see SVI.

SVI: spectral vegetation indices. Combinations of particular wavelengths of reflected solar radiation aiming at estimating the amount of vegetation present on Earths surface. Often satellite data is used.

TRAC: Tracing radiation architecture of canopies. An optical handheld instrument for estimation of canopy clumping for scales larger than shoots. See also Ω.

VI: vegetation indices. see SVI.

γ: Shoot-shading coefficient or needle-to-shoot area ratio (Gower and Norman, 1990). A clumping factor defining clumping in a forest canopy at shoot scale.

Ω: Clumping factor estimated by the TRAC instrument for scales larger than shoots.

6S model: A model used for atmospheric correction in FRT (see Vermonte et al. (1997))

Table of contents

1. Introduction

The leaf surface is site for gaseous exchange of CO_2, O_2 and H_2O between the plant and atmosphere. For a plant the rates of exchange are to an important degree controlled by the amount of leaf area present (Chen and Cihlar, 1996). Leaf area index (LAI) is a measure of the amount of leaf area defined as half the total leaf area per unit ground area (Chen and Black, 1992). LAI is found to be closely associated with important biological processes such as photosynthesis, evapotranspiration and carbon cycling hence as well as with important biological variables such as net primary production (NPP) (Chen and Cihlar, 1996; Cutini et al., 1998; Schlesinger, 1997). It is also a key input variable in spatial models of atmosphere and carbon cycling and in global circulation models (GCMs) (Chen and Cihlar, 1996; Chen, 1996; Law and Waring, 1994). In modelling attempts to describe and understand carbon cycling of sub-boreal and boreal forests reliable spatial LAI data (over these areas) are demanded (Eklundh et al., 2001). Data exists from passive remote sensors onboard earth orbiting satellites that retrieve spectral data of vegetation characteristics over large areas. This data might prove to be a solution achieving spatial LAI estimates to the models. Since leaves are strong absorbers of blue and red radiation, due to chlorophyll, and strong scatteres of near infrared radiation (NIR), several spectral vegetation indices (SVIs or VIs) using mainly the information in the red and NIR wavebands, and others, have been proposed aiming on being indicators of various vegetation characteristics on Earth's surface, among them LAI. In many studies LAI of boreal forests has been measured using ground based optical instruments like the LAI 2000 plant canopy analyzer (PCA) (Li-Cor inc., 1992) and tracing radiation architecture of canopies (TRAC) (Chen and Cihlar, 1995) and correlated with VI's using different types of regressions (eg. Chen and Cihlar, 1996; Eklundh et al., 2001; Eklundh et al., 2003). Using VI-LAI relationships to produce LAI surfaces over boreal forest areas to be used as model input data seems promising in theory but there are many factors affecting the nature and strength of such relationships. A major factor acting as noise in the relationships is the influence of radiation reflected by the forest floor (understorey, litter and soil combined) in this study mentioned as ground reflectance (Turner et al., 1999). Ground reflectance has been said to be the major problem when deriving LAI from satellite NDVI (normalised difference vegetation

index) for relatively open boreal conifer forests (Chen and Cihlar, 1996). This is quite understandable since the probability of seeing ground from vertical view in these forests may vary between 20-30% (Danson and Curran, 1993). In more closed canopies the influence of ground reflectance is lessened since the probability of seeing ground is decreased (Spanner et al., 1990).

To study the role of ground reflectance in forest reflectance forest radiative transfer models of different types has been applied in which a component of ground reflectance can be simulated (eg. Spanner et al., 1990; Gao et al., 2000; Kuusk et al., 2004).

1.2. Aim

The aim of this project is to investigate the influence of ground reflectance in VI-LAI relationships for deciduous and coniferous forests in southern Sweden by using a forest radiative transfer model. The model used is FRT (forest reflectance transmittance) version 09.2002 (Kuusk and Nilson, 2002) calibrated by field measurements from 20 forest stands. The VI-LAI relationships investigated are published in Eklundh et al. (2003) and based on Landsat TM data and ground based optical LAI measurements.

Specific objectives are:

1. To obtain theoretical estimates of the influence of ground reflectance on forest reflectance and VI's of boreal forests.
2. To estimate the influence of ground reflectance on LAI derived from satellite reflectance relationships.
3. To perform a sensitivity analysis of the sub model of ground reflectance in the context of FRT.
4. To find out if there exist any significant correlations between parameters of leaf and stand characteristics and LAI measured in field.

2. Theory

Earth observation satellites aim at obtaining valuable information about processes on the Earth's surface. This is mainly done by sensors on board the satellites measuring the radiance of the reflected sun radiation. When sun radiation interacts with a surface, some is absorbed, some transmitted and some reflected back towards space. The amount of absorption and reflection is dependent on the spectral properties of the surface. In the case of a forest the properties depend on spectral properties of individual material elements (leaves, woody material, soil), and their structure and orientation in space (canopy structure and spatial heterogeneity). Thus, Earth surface reflect spatial dependent unique combinations of radiation signals that can be detected by satellites orbiting Earth. However, before reaching a satellite sensor the radiation travels twice through the atmosphere, which causes a perturbation of the radiation signal known as the "atmospheric effect" (Kaufman, 1989, Vermonte et al., 1997).

2.1. The atmospheric effect

The atmosphere works as a remover and adder of information to and from the original reflected signal. The active processes are gaseous absorption, and scattering by molecules and suspended particles (aerosols) (Kaufman, 1989, Vermonte et al., 1997). Absorption is the process by which radiation energy is retained by a substance or a body (Barrett and Curtis, 1976). In the atmosphere, H_2O, O_3, O_2, CO_2, CH_4 and N_2O are the main gaseous absorption media, aerosols playing a minor role (Vermonte et al., 1997). Each of these gases absorbs radiation in specific regions of the solar spectrum. Thus, absorption reduces the amount of energy available at a given wavelength, making the surface target, as viewed by the sensor, seem less reflecting (Kaufman, 1989, Vermonte et al., 1997). Spectral bands used by satellite sensors viewing earths surface are usually located in spectral regions where most of the gaseous absorption is avoided, thereby minimizing its influence on the signal (Kaufman, 1989). These spectral regions are known as atmospheric windows.

Scattering occurs when radiation interacts with molecules and non-absorbing aerosols. The result is an immediate re-emission of the radiation in a direction other than the incident one (Campbell, 1996, Vermonte et al., 1997). The amount of scattering that

occurs depends on the sizes of the re-directors, their abundance, the wavelength of the radiation, and the depth of the atmosphere through which the radiation travels (Campbell, 1996). On the sun-surface path, a part of the radiation is back-scattered towards space, partly contributing to the total radiance recorded by the satellite sensor. It is thereby an interference term since it does not carry any information about the surface target (Campbell, 1996, Vermonte et al., 1997). The other part contributes in illuminating the ground as diffuse radiation. On the surface-sensor path, out-of-view scattering towards the sensor is an interference term if the surface is of non-uniform nature, which often is the case with a land surface (Vermonte et al., 1997). A part of the reflected radiation will be backscattered towards the surface and once again reflected towards space in the ”trapping effect” which acts as a small but significant interference term in satellite measured radiance values.

2.2. Structural and optical properties of leaves

To understand the spectral behaviour of leaves, knowledge about their chemical and structural properties is important. Typically, a leaf consists of several cell layers with characteristic biotical and spectral functions and properties (see figure 1). The uppermost cell layer is the epidermis, which consists of cells closely fitted together. Covering the epidermis is a thin wax layer, called the cuticle, which is semi-transparent and prevents the leaf interior from drying out (Campbell, 1996). The second layer is the upper mesophyll, made up by vertically elongated palisade cells. The cells have an interior of photosynthetically active chloroplasts composed of chlorophyll and other leaf pigments (f.e. carotenoids and xantophylls). Below is the lower mesophyll, consisting of irregular shaped spongy cells and intercellular air spaces. The lower epidermis completes the leaf structure, basically having the same structure and function as the upper counterpart. This layer is also containing the apertures of the stomates, each consisting of two guard cells. The guard cells determine the stomatal opening and thereby the amount of CO_2 present in the stomatal pores where CO_2 diffuses into the leaf interior to take part in the photosynthesis. Thus the stomatal opening is one of the factors determining the rate of photosynthesis (Schlesinger, 1997).

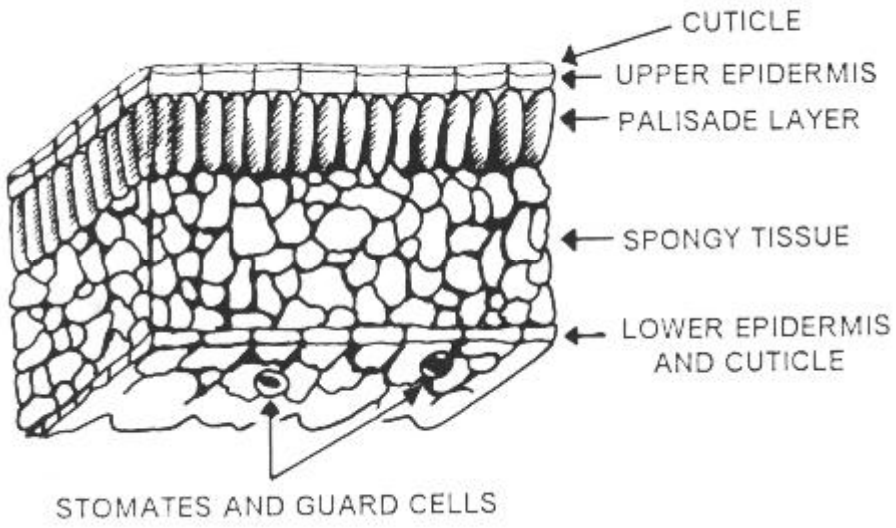

Figure 1: Schematic figure of a leafs interior. The palisade layer and spongy tissue is named upper and lower mesophyll in the text (www.lpl.arizona.edu/research/biosphere/Lesson/fig01.jpg).

In the visible domain (400-700nm), absorption of radiation by leaf pigments is the controlling factor leading to generally lower reflectances (see figure 2). Absorption by leaf pigment can be as much as 70 - 90% of the incident radiation, chlorophyll (a and b) being the main absorber(s) (Campbell, 1996). Chlorophyll absorbs radiation mainly in the red and blue spectral domains as a result of electronic transitions in its molecular structure, the leaf thereby appearing green in colour. About 10% of the radiation is reflected, the transmission component being slightly smaller. In the NIR (near infrared) region (700-1300nm) leaf structure explains the main optical properties, giving rise to strong scattering of the radiation (see figure 2). Typically the reflected part is about 50% and the transmitted about 50% of the incident radiation (Campbell, 1996). The single most important factor, giving rise to scattering is the number/amount of intercellular air spaces in the lower mesophyll layer, were the radiation is scattered at cell wall/air space interfaces (Campbell, 1996). Leaf pigments are almost transparent to NIR wavelengths and therefore absorption due to their presence is generally very small (Campbell, 1996). Water-related absorption is present in two minor bands in the NIR-region being centred at about 960 and 1100nm. Strong absorption by leaf water content characterizes the MIR (middle infrared) region (1300-2600nm) with absorption bands centred at 1450 and 1950nm (see figure 2).

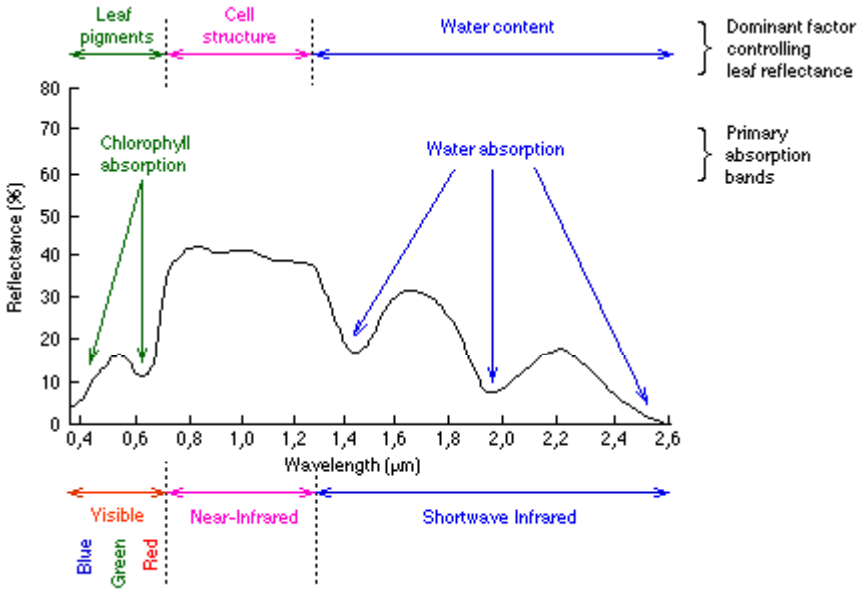

***Figure 2**: Typical reflectance response for vegetation with dominant factors controlling reflectance presented (http://www.cis.rit.edu/class/simg553_01/vegFig3.gif).*

Radiation interacting with a leaf is subject to the processes of absorption and scattering. Above scattering is described as reflection and transmission. However, these processes consist of two sub-processes each: Specular and diffuse reflection, and refracted and diffuse transmission (Goel, 1989). The reflection characteristics of a leaf can be described by the bidirectional reflectance distribution function (BRDF), and transmission similarly by the bidirectional transmittance distribution function (BTDF). The BRDF of a surface describes the reflectance for any set of view angles for a given illumination angle, and can be viewed as to which degree the surface approaches the idealized reflection behaviours of a total diffuse (Lambertian) or a total specular surface/reflector (Campbell, 1996).

2.3. Canopy reflectance

Scaling up to canopy reflectance (CR) (f.e. reflectance of a forest), other factors than those determining the optical properties of leaves must be taken into consideration. Canopy reflectance is a result of radiation interacting with a volume of vegetation elements (i.e. leaves, branches, stems, tree crowns, ground vegetation and understorey vegetation) and the ground surface (soil, bedrock, dead plant material). The elements have varying positions in space as well as different optical properties. However, the main factors determining canopy reflectance are those of the leaves. Leaves may vary

in size, shape, and angular distribution, giving each leaf a specific projected coverage of the ground surface. In the canopy, the upper leaves shadows the lower ones so that the total amount of their reflected radiation becomes a mixture from leaves that are sunlit and not sunlit. The shadowing effect decreases the canopy reflectance to 3-5% in the visible region and 35% in the NIR, which can be compared with reflectance values of 10 and 50% for single leaf, the relative decrease thereby being much lower in the visible region (Campbell, 1996). This difference is caused by the optical properties of the leaves, being good absorbers of visible radiation and good reflectors and transmittors of NIR. The amount of leaves present in the canopy volume is strongly affecting the canopy reflectance and also the extent of the shadowing effect. It is often described as the leaf area index (LAI). Initially, increased LAI leads to a decrease in canopy reflectance for the visible region and increase for the NIR region (Goel, 1989). The decrease and increase of CR with increased LAI is almost exponential until eventually saturating at LAI values around 2-3 for visible and 6-8 for NIR (Goel, 1989).

Optical properties of other vegetation elements, like the woody parts of branches, stems, trunks and whole trees (depending on scale), has little influence on canopy reflectance. However, they do determine the location of the leaves in the canopy at scales given by the typical size of the elements. Leaves are non-uniformly distributed in the canopy, e.g. they are clumped. The amount of clumping determines the probability of gap occurrence and the size of these gaps in the canopy and consequently the probability of radiation penetrating deeper into the canopy unaffected of scattering and absorption by leaves (Goel, 1989). The more clumped a canopy is the higher is the possibility of radiation reaching the ground. Clumping thus causes an inhomogeneous totally increased penetration of radiation trough the canopy at any level, compared with a hypothetical canopy where leaves are randomly distributed. In coniferous canopies the needles are generally positioned with higher structure in space than in deciduous ones (i.e. the needles are small, highly elongated and tightly fitted around the shoots and branches whereas leaves are generally bigger and having positions less dependent of shoots and branches). A coniferous canopy is therefore to a higher degree clumped than a deciduous one (Gower and Norman 1991).

Ground reflectance (sometimes called background- or understory reflectance) can be an important component in canopy reflectance (Goel, 1989, Spanner et al., 1990, Law and Waring, 1994, Nilson et al., 2001, Disney, 2002). The amount of visible ground surface reflecting radiation in the sensors viewing direction is mainly determined by the canopy-LAI and the degree of clumping at different scales in the canopy. The types of coverage determining the spectral properties of the grounds reflected radiation is generally of spatially non-uniform (patchy) nature. This is due to variations in light intensities, soil properties, moisture and other biotic and abiotic variables. These variables control the presence and absence of different types of vegetation, and thereby indirectly control the coverage of dead plant material (leaves/needles, twigs and branches), soil, and stone on the ground. The reflected spectral signature of the ground surface in a forest can be a complex mixture of many coverage specific signatures that may differ much from that of the actual canopy.

Angles of illumination and view also affect the canopy reflectance. The canopy reflectance can be described by a BRDF (see figure 3). As can be seen in figure 3 there is a distinct peak in reflectance when the canopy is viewed from the same angles as the solar radiation or close to. This occurs because there is a minimum proportion shadowed leaves and a maximum proportion sun-lit leaves viewed by the sensor. The phenomenon is called hot-spot.

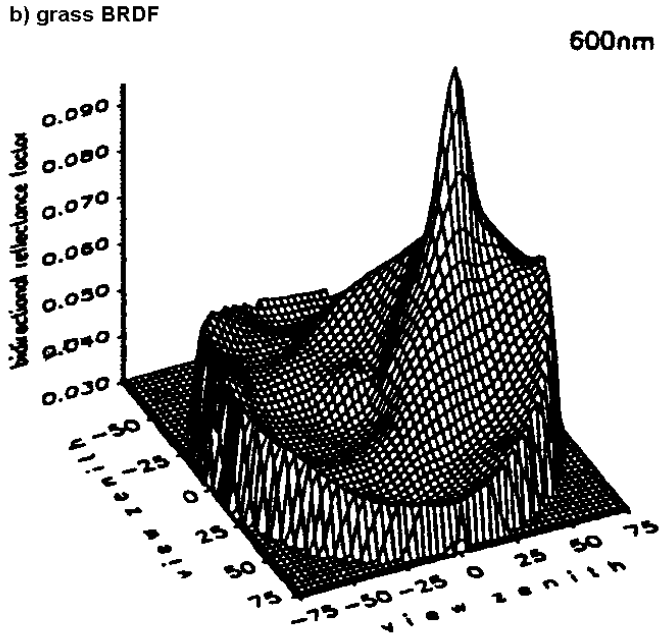

Figure 3: *A BRDF for a grass canopy at 600nm. The peak present in the right part of the figure is the hot-spot (http://cires.colorado.edu /~maurerj/albedo/grass_BRDF.gif).*

3. Modeling canopy reflectance

As can be concluded from the previous theory section there are numerous factors affecting the spectral signature of a forest canopy. Considering the reflectance (signal) from a canopy, ρ_{canopy}, at a given time it can be described as a relationship, R, of these factors (modified after Goel, 1989):

$$\rho_{\text{canopy}} = \text{R}(\lambda,\ \theta_s,\ \psi_s,\ \theta_o,\ \psi_o,\ \text{C}) \qquad (1)$$

Where

λ = wavelength

$\theta_s,\ \psi_s$ = solar zenith and azimuth angles

$\theta_o,\ \psi_o$ = view zenith and azimuth angles

C = a set of parameters representing the characteristics of the canopy and the underlying ground surface, f.e. spectral behavior of canopy elements and canopy structure.

This relationship is described by canopy reflectance (CR) models. A CR-model attempts to accurately describe the relationship R in order to predict the BRDF of a canopy, and, if possible, be able to determine parameters of C (e.g. LAI) with given values of $\lambda,\ \theta_s,\ \psi_s,\ \theta_o,\ \psi_o$, through a model inversion (Goel, 1989; Disney, 2002). When inverting, one searches the desired value(s) of C that best represents ρ_{canopy} by minimizing a merit function (for further information see Press *et al.* 1992, p. 498). There are several different approaches in mathematical CR-modeling. Often they are broadly divided into four model categories (modified after Goel, 1989; Disney, 2002):

1. *Empirical models*. Here, canopy reflectance (CR) is described by a polynomial function. The function in question should not be related to any of the physical properties of the system under observation (Disney, 2002).

2. *Physically-based models*. Here, the canopy is described as a physical structure having optical properties of the canopy elements. The models describe the radiatiative behavior within these structures using functions that approximate the scattering processes of a canopy. On this basis the CR can be calculated. In one

type of models, called geometrical optical models (GO-models), the canopy is described as geometrical objects (cylinders, cones, ellipsoids). Reflectance properties of four components are described separately in such models. These are, sunlit crown, shadowed crown, sunlit ground and shadowed ground. Under the assumption of parallel ray geometry (direct sunlight) the proportions and subsequently the reflectance factors of the four components are calculated for the view angle(s) given that size, density and distribution of the geometrical objects are known (Disney, 2002). Finally, the reflectance factors of the four components are summarized in a special manner to obtain CR.

In another type, called turbid medium models, the canopy is described as a uniformly thick semi-transparent layer above the ground containing canopy elements of a known distribution and density (Goel, 1989). Within this layer the photon interactions with the canopy elements are described mathematically using integrals and differential equations based on radiative transfer (RT) theory (originating from the works of Chandrasekhar (1953; 1960) in (Disney, 2002)).

There are also models combining the approaches of the two previously mentioned types of physically based models, so called hybrid models. In such a model, the trees of the canopy are described as geometrical shapes. Within these shapes the reflectance is described using radiative transfer theory.

3. *Computer simulation models*. Here, the whole canopy structure is described in 3D with some level of geometrical realisticity (including trees, stems, branches, shoots, leaves etc.). All canopy elements have specified optical properties. The model calculates the interactions of rays of radiation illuminating the canopy. Scattering behaviors following each interaction with a canopy element, due to its optical properties and position in space, is also calculated (Disney, 2002). In this way the spectral amount of reflected radiation traveling from the illumination angle to the view angle via the canopy can be calculated.

4. *Semi-empirical (kernel-driven) models*. This type of models uses a combination of the empirical and physical approaches to describe canopy reflectance. It is assumed that scattering from a heterogeneous surface is composed of separable scattering components, called kernels (Disney, 2002). Each kernel describes a particular component of the canopy scattering behavior solely empirical or physical, or

combined (f.e. single scattering of sunlit leaves, scattering of diffuse sky radiation, multiple scattering within the canopy). Finally, the calculated values of the kernels either are multiplied or added to each other in order for the model to present its estimated value of the canopy reflectance (Disney, 2002).

3.1. The Forest Reflectance Transmittance (FRT) Model

The first version of the FRT model is described in Nilson (1990) and Nilson and Peterson (1991). With time the computer code algorithms have been modified and sub-models added for calculation of leaf optics, PROSPECT (Jacquemoud and Barret, 1990; Jacquemoud et.al., 1996), ground reflectance, MCRM (Kuusk, 1995) and later MCRM2 (Kuusk, 2001), and atmospheric radiative transfer, 6S (Vermonte et.al., 1997). FRT Version 09.2002 is used in this project. It is a physically based model of the hybrid type, i.e. it has the properties of both geometrical optical and radiative transfer based models (see model category 2 in part 3). FRT calculates bi-directional reflectance in the 400-2500 nm spectral region at a maximum spectral resolution of 1 nm. In the model the trees of a forest scene are mathematically described as geometrical volume elements. Crowns are described as ellipsoids or cones, and trunks as cylinders. On the ground a homogeneous layer of vegetation is present (modeled by MCRM2), and below it a homogeneous soil surface represented by weights of Price (1990) four basis functions of soil reflectance. Trees of the scene can be divided into classes judging by size, species, or group of species. Within each such class trees have identical geometrical and optical properties.

In a simplified manner, it can be said that for radiation entering the forest canopy, PROSPECT calculates reflectance and transmittance for the green vegetation and the FRT algorithm modifies these values to represent the whole canopy (its different elements, and structure). The transmitted radiation is again modeled by PROSPECT in the same manner but this time for the ground vegetation. The MCRM2 algorithm modifies these values to represent the reflectance of the forest floor. FRT then calculates the final canopy reflectance taking the reflected radiation of the forest floor into consideration.

3.1.1. Calculation of Reflectance in FRT

Below follows the calculation of reflectance in FRT after the FRT manual (Kuusk and Nilson, 2002) added with extra explanations.

The model calculates the bi-directional reflectance of a forest canopy for a given set of view and illumination angles by describing four reflectance factors acting on the incident flux of radiation:

$$\rho_{canopy} = (I / Q) * (\rho_{CRi}(r_1, r_2) + \rho_{GRi}(r_1, r_2)) + \rho_{CRd}(r_2) + \rho_{GRd}(r_2) \quad (2)$$

Where

I = direct down-welling flux

Q = total down-welling flux (Q = I + D, where D is the diffuse flux)

ρ^{i}_{CR} = single scattering of direct radiation in tree crowns

ρ^{i}_{GR} = single scattering of direct radiation on ground

ρ^{d}_{CR} = scattering of incident diffuse radiation and multiple scattering in tree crowns

ρ^{d}_{GR} = scattering of incident diffuse radiation and multiple scattering on the ground

(r_1, r_2) denotes that the radiation traveling from the direction (r_1) given by the illumination angles, into the direction (r_2) given by the view angles. For ρ_{CRd} and ρ_{GRi}, being diffuse reflectance factors, only radiation traveling in direction r_2 is of interest.

Radiation from single scattering events usually makes up a larger portion of the reflected radiation than those due to diffuse scattering in the optical domain of the electromagnetic spectrum. Accordingly, single scattering (ρ^{i}_{CR} and ρ^{i}_{GR}) is modeled to a higher detail than diffuse (ρ^{d}_{CR} and ρ^{d}_{GR}).

The reflectance factor of single scattering of tree crowns is calculated separately for each tree class and then summarized to ρ^{i}_{CR}. Considering a forest consisting of one tree class having ellipsoid tree crowns, ρ^{i}_{CR} is calculated according to:

$$\rho^{i}_{CR} = t_d\, c \iiint_V u \cdot \Gamma(r1, r2) \cdot p00(x, y, z; r1, r2) dx dy dz / \cos\theta \qquad (3)$$

Where

t_d = tree density (number of trees / unit ground area)

c = tree distribution parameter

u = area volume density of foliage elements (leaves and branches) within the crown

$\Gamma(r_1, r_2)$ = scattering area phase function of the foliage elements describing the angular distribution of scattering from direction r_1 to r_2

$p_{00}(x, y, z, r_1, r_2)$ = the bi-directional gap probability, or the probability of existence of free lines of sight, from r_1 to r_2 in position M=(x,y,z) in the tree crown.

$\cos\theta$ is a factor accounting for the reduced amount of radiation, present on the surface where point M is, for increasing illumination (solar) zenith angles (θ) (Disney, 2002); V stands for the volume of the ellipsoid.

Gap probability is calculated for all the points M that have a regular distribution over the canopy ellipsoid. The positions of the points M on the crown are given by a cubature of the ellipsoid.

The bi-directional gap probability $p_{00}()$ is the product of two separate components, p_1 and $p_2.p_1$ describes the gap probability for the crown and p_2 the between crown gap probability for the path outside the crown. In the calculation of p_1 hot spot correction in the viewing direction as well as LAI and BAI in the crown volume is accounted for. For more information and detailed information about the calculation of p_1 and p_2 see appendix 1 and Kuusk and Nilson (2000).

The reflectance factor due to single scattering on the ground, ρ^{i}_{GR}, is calculated as the product of the gap probability p_2 and the total reflectance factor for the ground calculated by the MCRM2 sub model for ground reflectance. p_2 is calculated for the ground level where $z_1 = z_2 = l_{12} = 0$.

The diffuse reflectance factors due to multiple scattering and scattering of diffuse sky radiation in the view direction, ρ_{CRd} and ρ_{GRd}, are calculated using a four-flux approximation to the radiative transfer equation (Disney, 2002). The four fluxes

considered are: Vertical upward flux, vertical downward flux, direct solar flux, and flux in the viewing direction. Each flux is defined by a differential equation that can be solved analytically (general solutions are given in Bunnik (1978)). MCRM2 is used for computation of some of the ground reflectance parameters needed for calculations of the diffuse fluxes. It also uses the four-flux calculation procedure, in this context and when run separately. For further reading, see Kuusk (2001).

3.2. MCRM ground reflectance model

The ”Multispectral Canopy Reflectance Model” (MCRM) is a physically based CR-model of the turbid medium type (see model intro section) developed by A. Kuusk at Tartu Observatory, Estonia, first presented in Kuusk (1995). The model simulates directional reflectance for a uniformly thick semi-transparent layer of vegetation and an underlying homogeneous soil surface in the spectral region of 400-2500nm at a maximum resolution of 1nm (equal to FRT). Optical properties for green vegetation elements are described using PROSPECT2 (Jacquemoud and Barret, 1990; Jacquemoud *et al*., 1996), and for soil by using weights of Price’s (1990) four basis functions of soil reflectance respectively. Structural parameters of the canopy are given by the LAI, linear leaf size, and two leaf angular distribution (LAD) parameters. The spectral distribution of direct and diffuse solar radiation at top of canopy level in the models working region (400-2500nm) is calculated using functions defined by McCartney (1978). A typical infile with parameters is given in appendix 2.

In FRT version 09.2002 (used in this project) MCRM’s successor, MCRM2, is used for calculation of ground reflectance. MCRM2 is different from MCRM in the way that a second thin vegetation layer is present on the ground surface below the uniformly thick vegetation layer. Calculation of reflectance in MCRM2 is basically the same for each of the two layers as in MCRM and each layer has the same set of input parameters as in MCRM.

3.2.1. Calculation of reflectance in MCRM2

Below the calculation of reflectance is roughly described for MCRM2 following Kuusk (2001).

The directional spectral reflectance is calculated as the sum of single scattering of direct solar radiation and the diffuse flux:

$$\rho = (S / Q)\ \rho_1 + \rho_d \qquad (4)$$

Where

ρ = directional reflectance

S = direct solar spectral irradiaces

Q = total spectral irradiances

ρ_1 = single scattering component

ρ_d = diffuse flux in the viewing direction

The single scattering component (ρ_1) is the sum of single scattering from the two vegetation layers and the soil layer:

$$\rho_1 = \rho_1^{c1} + \rho_1^{c2} + \rho_1^{soil} \qquad (5)$$

Where

ρ_1^{c1} = single scattering component, upper vegetation layer

ρ_1^{c2} = single scattering component, lower vegetation layer

ρ_1^{soil} = single scattering component, soil surface

For further information on the calculations of single scattering components of the vegetation layers and soil see appendix 1.

Calculation of diffuse reflectance is done using the same four-flux approximation to the radiative transfer equation as in FRT. For further reading see Kuusk (2001).

3.3. PROSPECT leaf optical model

PROSPECT (Jacquemoud and Barret, 1990; Jacquemoud *et al*., 1996) is a radiative transfer model of the empirical type (see CR-modeling above) which calculates the hemispherical reflectance and transmittance of a leaf in the range 400-2500 nm using a leaf mesophyll structural parameter (N) and concentrations of leaf chemicals (such as chlorophyll A and B, lignin, cellulose, leaf water etc.) as in-parameters. Scattering is modeled by weights of the N-parameter and the refractive index of leaf chemicals, while absorption is modeled by weights of absorption coefficients of the leaf chemicals (Jacquemoud *et al*., 1996). The model is incorporated as a sub-model in FRT and MCRM for modeling leaf reflectance and transmittance and can be inverted fast by use of a reflectance spectrum (ρ_{canopy}), to retrieve concentrations of leaf chemicals (C).

4. Optical instruments

Below follows information about the optical instrument used in the field study presented.

4.1. Li-Cor LAI-2000 Plant Canopy Analyzer

Various techniques have been developed to estimate forest LAI. Destructive field measurements is perhaps the most accurate one, but the values obtained are only representative for the measurement area and depends upon extrapolation by the use of allometric equations if used for larger areas (Chen et al., 1997). Another direct method, applicable for deciduous species, is litter collection using litter-traps. Here, the LAI for a stand is estimated through empirical relationships between leaf dry weight and leaf area (Chen et al., 1997; Eklundh et al., 2003; Eriksson et al., 2005). In general, direct methods are labor intensive and do not always provide accurate LAI-estimates, furthermore, it is difficult to follow the spatial and temporal development of LAI throughout the growing season (Cutini et al., 1998).

LAI can also be estimated using indirect methods. These methods are based on the measure of light transmission through canopies. Instruments have been developed that provide rapid LAI estimates, amongst others the LAI-2000 Plant Canopy Analyzer (PCA) (Li-Cor, Inc., Lincoln, NE, USA). When using the PCA to estimate LAI, diffuse light intensity is measured above and below the canopy simultaneously using two identical instruments. The instrument projects the radiation on to five sensors arranged in concentric rings that measures the light intensities in the range 320-490nm for five respective view angle sectors (0-13°, 16-28°, 32-43°, 47-58°, and 61-74°) by use of a fish-eye lens (Li-Cor, 1992). The fraction of non-intercepted radiation, analogous to transmittance through the canopy, can then be calculated for each of the view angle sectors as given in the PCA instruction manual (Li-Cor, 1992):

$$T(\theta_i) = \textit{diffuse intensity above canopy / diffuse intensity below canopy} \quad (6)$$

Where:

$T(\theta_i)$ = The probability of non-interception by foliage as radiation passes through the canopy at view angle θ_I (i = view angle sector 1 – 5), also called gap fraction.

The five gap fraction values are used in a relationship based on Millers Theorem (see (Miller, 1967)) to calculate the LAI (for further information see PCA instruction manual (Li-Cor, 1992)):

$$LAI = 2 \sum_{i=1}^{5} -\ln(T(\theta_i))\, cos(\theta_i)\, w(\theta_i) \qquad (7)$$

Where:
θ_i = view angle for ring no. i
w = constant weighting factor

The LAI estimate is however correct only if some assumptions are met (Li-Cor, inc., 1992):

- The leaves act as perfect absorbers in the sensor spectral range (320-490nm). No reflection or transmission occurs when radiation interacts with a leaf, which thereby appears ”black” to the sensor.
- The foliage is randomly distributed.

In reality, none of these assumptions are met. The leaves are not perfect absorbers in the specified spectral range, even though they absorb most of it appearing ”dark grey” to the sensor, and foliage is never randomly distributed but is clumped from shoot, branch to crown level. Further, woody canopy elements (branches, stems) also act as absorbers of the radiation. Because of these reasons, the LAI estimate given by the PCA actually is a product of the plant area index (PAI) (area index of all canopy elements) and a clumping factor (Ω) and has been given the name ”effective LAI” (L_e) (Black et.al., 1991; Chen et.al., 1997). For random foliage distribution, Ω is unity ($\Omega = 1$), for clumped $\Omega < 1$, and regular $\Omega > 1$. Since light transmission is higher for clumped canopies than for random ones, in reality having the same LAI, L_e yields an underestimate of LAI for clumped canopies, especially if these have an open

structure (i.e. spaces between the crowns) (Gower et.al, 1999). This clumping effect is more pronounced for conifers (Li-Cor, Inc., 1992, Chen et.al., 1997). The underestimation might be reduced when compensating for the contribution of woody material area in the PAI. However, leaves often mask stems and branches, thereby lessening their participation in PAI (Gower et.al., 1999).

4.2. TRAC theory

TRAC stands for ”Tracing Radiation and Architecture of Canopies” and is a hand-held optical instrument that measures sun-fleck width below the canopy for estimation of the canopy gap size distribution. This is done in sunny weather by walking at a slow and steady pace (about 0.3 m/s) along a transect with the instrument, that obtains measurements of the through canopy transmitted visible radiation intensities at a frequency of 32Hz (Leblanc et.al., 2002). The measurements yield a gap size distribution and an estimate of the gap fraction (transmittance, (see PCA-part)) for the canopy above the transect. This distribution is compared with a theoretical gap size distribution for a canopy with random foliage distribution (see Miller and Norman, 1991). With knowledge of the sun zenith angle and theoretical gap size distribution for a canopy with random foliage distribution, all gaps in the measured distribution existing because of clumping of foliage elements in the canopy can be compensated for using a calculation procedure developed by Chen and Cihlar (1995). After compensation a new gap fraction estimate can be calculated. The difference between the original and new gap fraction can be used to achieve an estimate of the clumping factor (Ω) (Leblanc et.al., 2002). The estimate can then be used to correct a L_e-value (measured for the same canopy) to achieve a theoretically more correct LAI estimate.

For detailed information about calculation procedures and other theory used by TRAC, see Chen and Cihlar (1995); Chen, (1996); Chen et.al., (1996); Leblanc et.al., (2002).

4.3. LAI and LAI-estimates

As mentioned above (see, PCA part) LAI-values estimated by the PCA (L_e) are only true under special occasions, which seldom (if ever) are met in reality. However, corrections for canopy clumping at different levels and radiation interception by woody parts can be made for L_e-estimates that yield better approximations closer to the actual LAI of a canopy.

Conifer needles are clumped on shoots making needles shade each other more than is the case in a random canopy. This can be corrected for by multiplying the L_e-value with a conversion factor (γ) called shoot-shading coefficient or needle-to-shoot area ratio (Gower and Norman, 1990; Chen, 1996). This LAI-estimate is called L_{Gower} and is stated as:

$$L_{Gower} = L_e * \gamma \qquad (8)$$

The correction is only valid for conifers, since γ equals 1 for broadleaf species (Eklundh et al., 2001). This is the case since broadleaf canopies are randomly distributed at shoot level (ibid.).

The vegetation elements are still clumped at higher canopy levels (from branch level to spatial distribution of crowns) and participation of woody parts may still be present. Chen (1996) has suggested a LAI estimate where all of the mentioned factors (WAI, γ and Ω) are corrected for:

$$L_{Chen} = L_e (1 - \alpha) \gamma \ / \ \Omega \qquad (9)$$

Where

L_e = Effective LAI as estimated by PCA

α = WAI / PAI where WAI is the woody area index and PAI is the plant area index

γ = needle-to-shoot area ratio

Ω = clumping factor estimated by the TRAC instrument

There are several other LAI-estimates existing but L_e, L_{Gower} and L_{Chen} are all used in this project.

4.4. ASD spectrometer: FieldSpec® Handheld

Spectrometers are used to study radiative properties of various targets under controlled laboratory conditions as well as in the field. They measure radiation intensities at a given number of wavelengths distributed regularly over a part of the electromagnetic spectrum. Measurement results in a spectrum of radiative entity/unit wavelength. Usually reflectance properties are studied.

In this study the ASD spectrometer FieldSpec Handheld was used. The spectrometer has a 25^o field of view and is active in the spectral range 325-1075 nm. It has a sampling interval of 1.6nm (325-1075nm) and a spectral resolution of 3.5nm at 700nm. FieldSpec Handheld can record a reflectance spectrum in 17 milliseconds and can be set to record mean value spectra under user selectable integration times. Thereby errors associated with clouds and winds under solar illumination are minimized. It is connected to a notebook PC using a serial port and is run via a specific processing program.

A measurement starts with selecting an integration time defining the number of spectra measured making up the final mean value spectra. Measurement of the sensors systematic noise (SN), called dark current, is then performed. The instrument shutter is automatically closed during this measurement. Following this is a measurement of a white reference spectrum using a reference plate with near Lambertian or diffuse reflectance properties. The measurement is done in a place with similar illumination as the target (as close as possible to where the target is). A measurement represents the total incoming intensity of radiation in each of the individual sensors. After this the reflectance of the target is measured. Each sensors reflectance factor is then computed as follows:

$$R(\lambda) = (\text{target signal - SN}) / (\text{white reference signal – SN}) \qquad (10)$$

Where:

$R(\lambda)$ = computed reflectance of each individual sensor

The reflectance values/factors and wavelength are the plotted versus each other creating a spectrum of reflectance (see figure 2).

5. Background

5.1. Forest study areas and stands

The stands selected for the study are located in six forested areas within 30 kilometers distance north east to east of Lund: Skarhult, Fulltofta, Vomb, Skrylle and Linebjer, (see figure 4).

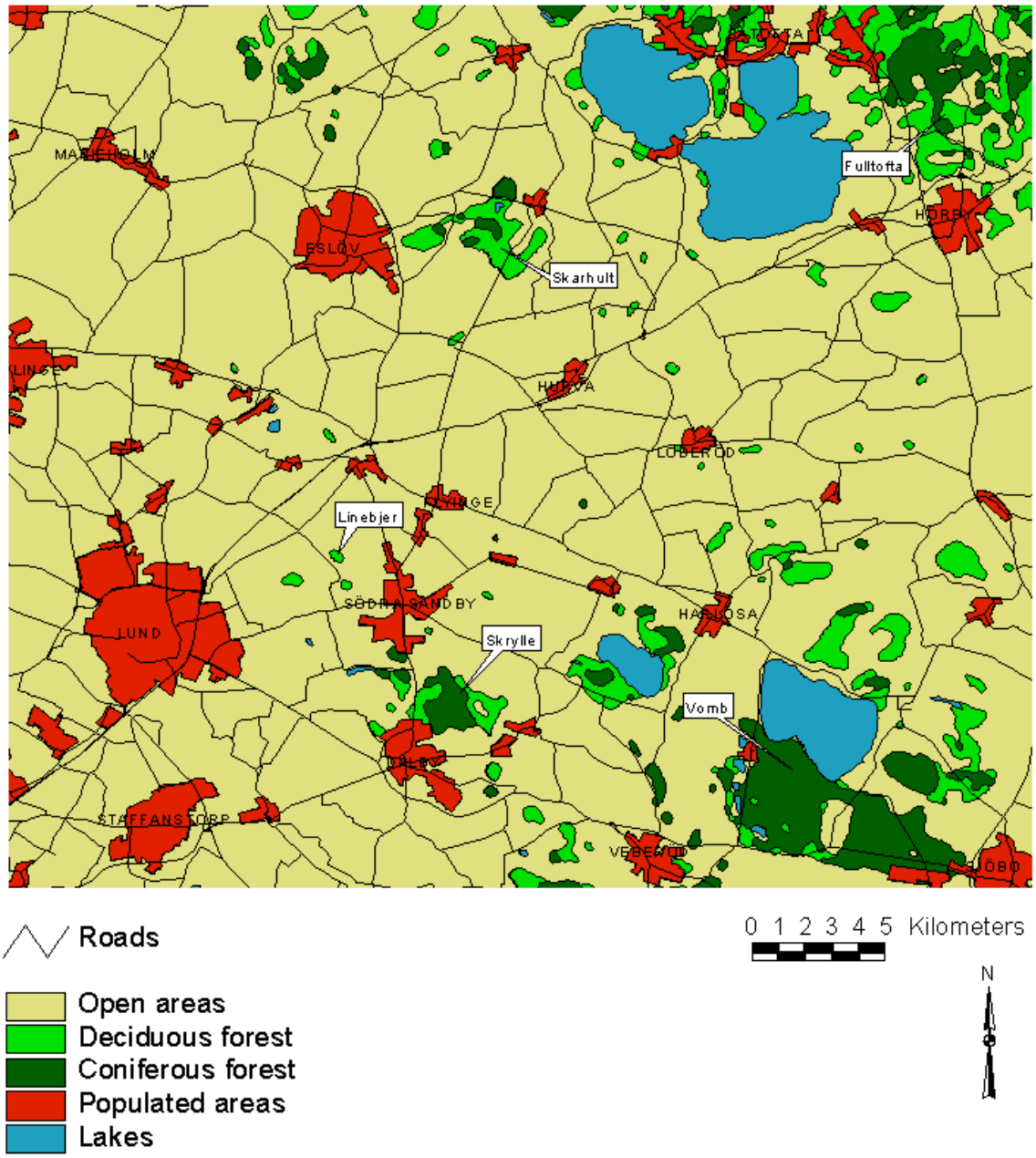

***Figure 4**: Map over location of the forest areas.*

A few years back, forest stands for conducting measurements in a Ph.D.-project were set up by Ph.D.-student Helena Eriksson and supervisor Ph.D. Lars Eklundh in the Skarhult and Fulltofta forest areas. Seven of these stands were used in this study (see Appendix 3). Main focus of the study was on deciduous forest, but some coniferous forest was also to be included. 14 deciduous and 6 coniferous stands were said to be a reasonable allotment to collect data from. A description of the stands in their respective areas, in respect of main- and sub-species and ground cover is presented in appendix 3. Stands were selected according to the following criteria:

- The stand had to be approximately 90 x 90 m with relatively homogenous tree and stand structure.
- The different stands had to represent a visual variation in canopy closure and amount of ground vegetation.
- The ground surface had to be horizontal, or close to.
- The stands had to be reachable within 30 minutes of driving, starting from Lund.
- As many stands as possible made up of single species had to be found, focusing on beech and oak.
- The stand had to consist of either deciduous or coniferous species.

5.2. Instruments and data

The following instruments, models and computer programs were used in the study.

Instruments:

- Crown radius meter
- Clinometer (Suunto)
- Gridded square: Aluminium framed square covering 0.5 m^2 with 5 X 5 smaller squares inside. Each minor square is then covering an area of 4% of the total gridded square area.
- Tape-measure, 50m

- Magellan differentiated GPS.
- TRAC (Tracing Radiation and Architecture of Canopies). See theory chapter and TRAC manual Version 2.1 (Leblanc et.al., 2002).
- LI-COR, LAI 2000 Plant Canopy Analyzer: See theory chapter and LI-COR LAI2000 Plant Canopy Analyzer manual (LI-COR corp., 1992).
- CANON IXUS II: 3.2 Mpix digital camera
- FieldSpec HandHeld Spectroradiometer from ASD (Analytical Spectral Devices)
- Rod secateur. Length: 4m.
- Dedolight DLH2 105W NV-halogen photo lamp with 12V DC (direct current) power supply.

Models and computer programs:

- Forest Reflectance Transmittance Model, version 09.2002. For information, see chapter 3.1, Peterson and Nilson (1991), Kuusk and Nilson (2000), Kuusk and Nilson (2002).
- MCRM (Multispectral Canopy Reflectance Model): See chapter 3.2, Kuusk (1994).
- MCRMinverted (Kuusk, 1995)
- Prospect Leaf Optical Properties Model (Jacquemoud et.al., 1996)
- PROSPECTinverted, (Kuusk, 1996)
- ANGLES: Program used to calculate sun zenith angles. Written by Ph.D. L. Eklundh.

6. Method

The investigation began with field measurements in the stands where raw data of the stand characteristics, considering structural and optical properties, were collected. From the raw data FRT model parameters were obtained through calculations, separate inversion of the MCRM and PROSPECT models, and analysis of data from the optical instruments (PCA, TRAC, ASD spectrometer). Infiles were created and the FRT model was run, resulting in a set of reflectance spectra for all stands from which reflectance in bands corresponding to Landsat TM 1-4 was calculated. Finally a statistical analysis was performed on the reflectance data together with measured LAI values and various modeled stand parameters. A flow chart showing the different steps of the method is presented in Figure (5).

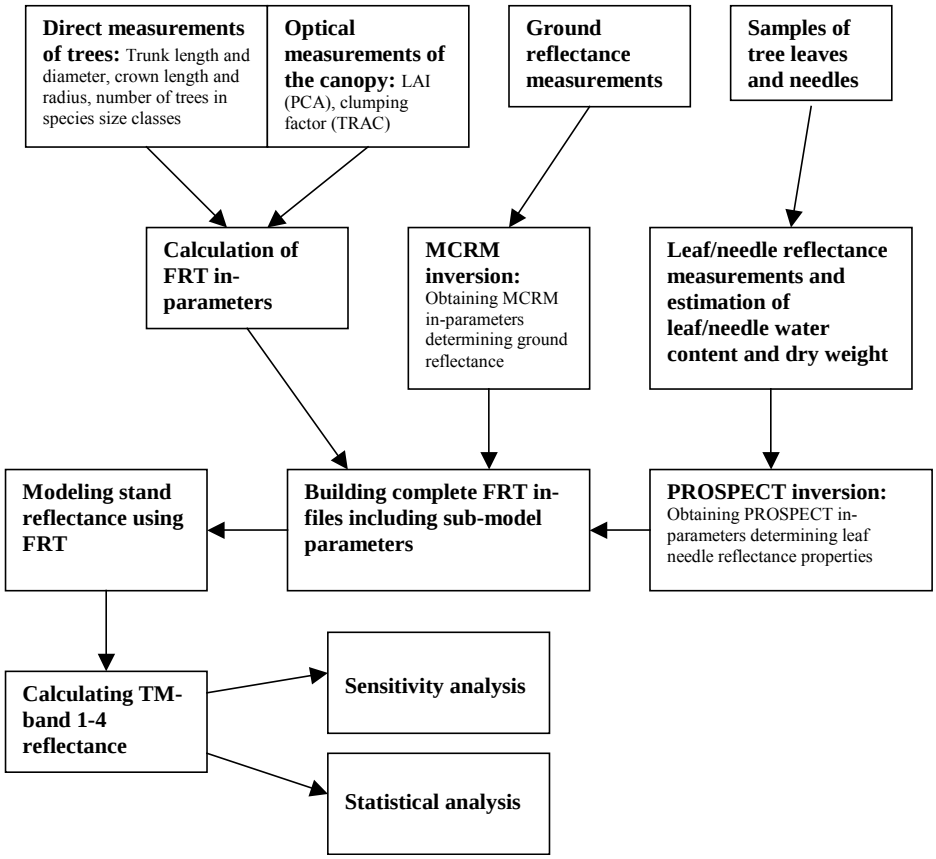

***Figure 5**: Flow chart showing the general steps of the method.*

6.1. Fieldwork

The fieldwork was carried out from mid-June to early September 2003, thus covering the peak of the forest growing season. The considerable length of the fieldwork period was due to weather dependent measurements with the LAI 2000 and TRAC instruments, the desired number of 20 stands to identify and conduct measurements in, and the late possibility to collect leaves for estimation of leaf chemical and optical properties (25:th of August and 1:st of September).

For a typical stand, a sampling plot of 30 x 30 m in the stand center was selected to conduct measurements in. A GPS point was taken in the mid-point. In the sampling plot the number of trees in the tree size classes for the existing species were visually determined according to the division in circumference (c): Large $c > 50$ cm, medium $50 = c \geq 30$ cm, small $30 = c \geq 10$ cm.

For three representative trees in each species size class a set of structural parameters were estimated. DBH (Diameter at Breast Height) was derived from trunk circumference measurements at approximately 130 cm height using a measuring tape. Crown length and tree height was derived using an inclinometer, and the radius of the visually appreciated thinnest and widest crown diameters on each tree were measured using the "crown radius meter". The "crown radius meter" consists of a small, towards the holder, angled mirror fixed on top of a metal rod with a vertical fixed metal plate a few centimeters above it. The instrument is held with a handle, connected to the rod via a gyro so that the rod is always vertical and the mirror reflects vertical downward light towards the operator. When measuring a crown radius the holder looks into the mirror so that the vertical metal plate is viewed as a thin line in the reflection of the above tree crowns. When the thin line is positioned on the radius (edge) of the crown, one sticks the rod into the ground. The crown radius is then the distance from the rod to the tree trunk.

In sunny weather, the TRAC instrument was used for estimation of the canopy-clumping factor (Ω). For the measurement to be correct the sun zenith angle had to be smaller than 40^{o}. The measurements were done in three parallel 30 m transects with approximately 10 m spacing, perpendicular to the sun azimuth. The middle

transect was located over the center of the stand. In cloudy weather, measurements of the effective LAI were carried out with the Li-Cor LAI-2000 PCA instrument. Two sensors mode was used, one sensor measuring under open sky view on a nearby field and the other below the canopy (for further information see Li-Cor (1992)). About 40 PCA measurements were taken in each stand.

The ground cover was studied along a 30 m transect centered over the stand mid-point. At ten points with 3 m spacing, starting from one end of the transect, a girded quadrat was laid out and a digital photo of the quadrat taken. The type of ground cover present in the quadrats was visually divided into percentage vertical projected coverage of pre-defined ground type categories (see table 1). A spectrum of the ground reflectance for the quadrat area (diameter ≈ 0.5meter) was also taken using the ASD spectrometer measuring at a height of 1 meter. Before each such measurement, a white reference on a near-lambertian plate was performed adjusting the ground reflectance measurement to the *in situ* light conditions (for further information see ASD spectrometer part). In the five stands with most ground vegetation present (L1, L2, L4, L5 and L6) a ground vegetation study for estimation of SLW (Specific Leaf Weight (g/m^2)), EWT (equivalent water thickness (cm ≈ g/m^2), a measure of water content) and LAI, was performed using destructive sampling in 20x20 cm areas. Five visually representative samples per stand were taken.

***Table 1**: Ground cover categories*

Ground cover categories
Grasses
Herbs
Brushwood
Bushes
Ferns
Mosses and lichens
Dead leafs
Dead branches and twigs
Dead conifer needles
Soil
Stone

FRT uses the PROSPECT model to simulate leaf reflectance. Therefore, estimation of PROSPECT leaf chemical parameters determining the optical properties of the leaves

was needed. Only EWT and SLW were subject to estimation based on measurements of stand leaf samples, thereby making it possible to obtain the PROSPECT N parameter and the parameter of leaf chlorophyll concentration (cAB (microgr./m^2 leaf area)) needed in FRT by running PROSPECT in inverted mode. For the PROSPECT inversion SLW and EWT were estimated in eight stands for the species:

- Birch (*Betula spp.*): L1
- Oak (*Quercus Robur*): L2, L4
- Spruce (*Picea abies*): L8
- Pine (*Pinus sylvestris*): L9
- Beech (*Fagus sylvatica*): L10, L11, L14

The stands were selected so that they represented different stand structures, as for beech and oak, or to be representative for their tree category (i.e. Birch, Spruce and Pine). In a stand, one representative tree was selected and two samples of leaves or needles were taken; one from high directly sun-lit branches, and one from low shadowed branches. In the laboratory, spectra of one layered leaf/needle reflectance were taken using the ASD spectrometer: One times ten leaves per sample, and one times as many year-shoots as could be determined on a conifer branch. Measurements were done under controlled conditions using a photo lamp as a constant light source (see figure 6). All samples were weighed and sample leaf/needle area was determined using a photo scanner. Samples were then dried (in a drying-oven) for 48 h at 75 ^{o}C for all water to dry out after which dry weights were determined. SLW and EWT mean values of sun and shade samples were then calculated for the tree categories and used together with mean value spectra of one layered leaf/needle reflectance in PROSPECT inversions to obtain the rest of the desired parameters.

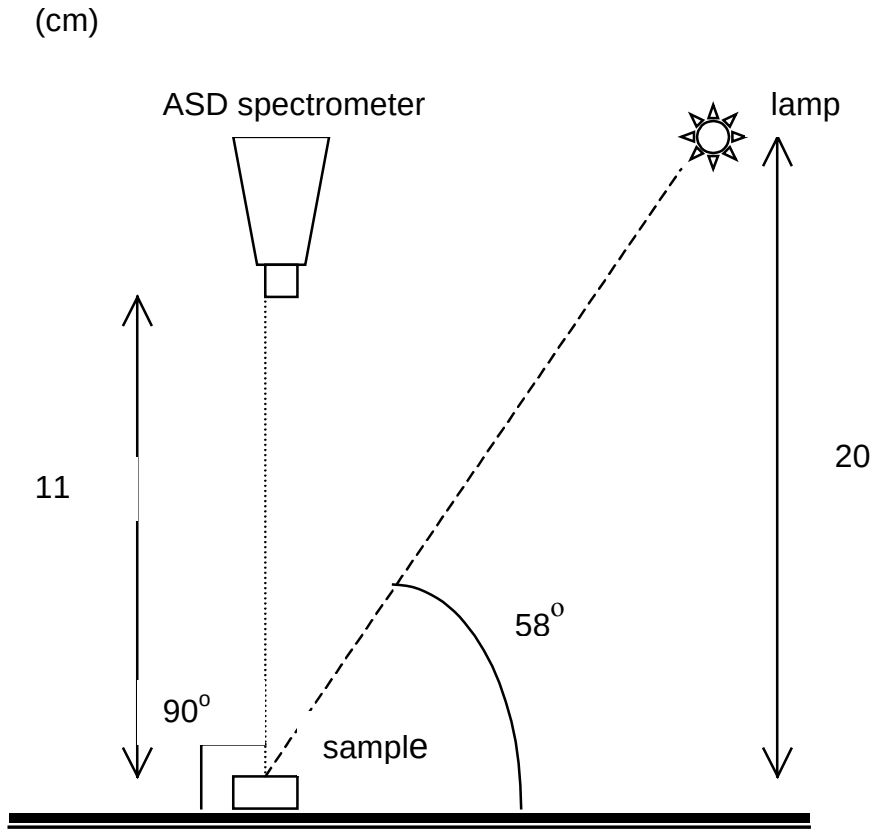

***Figure 6**: Schematic figure of the leaf measurements*

6.2. Determination of FRT model parameters

To assess the possible effect of variation in ground reflectance on LAI in LAI vs TM reflectance relationships using FRT, model parameters representing maximum and minimum ground reflectance were to be estimated for the stands. Ground reflectance being the studied variable, the other parameters were held constant and thereby estimated once per stand. Accordingly, two sets of ground reflectance parameters and one set of other parameters were to be estimated for a stand, resulting in two FRT

input files per stand, one representing maximum ground reflectance and one minimum. The ground reflectance parameters were estimated by an inversion (see model inversion part 3 page 13) of MCRM. PROSPECT was also inverted for obtaining leaf chemical parameters. The other FRT parameters were partly calculated from measured stand data, partly taken from literature or held constant using model default values.

6.2.1. Treatment of reflectance spectra measured with the ASD spectrometer

Reflectance spectra were needed when inverting PROSPECT and MCRM. Due to noise in reflectance values in the beginning and end of the spectra, the usable data generally was in the range 400 - 1000 nm. Spectrum raw data, as registered by the spectroradiometer, was in a discontinuous nm/step series and needed to be converted to a 5nm/step series in order to be used in the inversions. A MATLAB program using a ”nearest neighbor” approach was constructed for conversion to 1nm/step series, where after 5nm/step series were created.

6.2.2. MCRM inversion

Spectra of ground reflectance representing maximum and minimum ground vegetation for a stand were visually selected according to the criteria:

Maximum: The spectrum showing sharpest ”red edge” and highest over-all reflectance values.

Minimum: The spectrum showing flattest ”red edge” and lowest over-all reflectance values.

By red edge is meant the steep increase in reflectance in the red part (close to <700nm) of a typical vegetation spectrum (see figure 2, page 9). Occasional spectra showing abnormal configuration and much noise, when compared to the other spectra measured in the same stand, were excluded.

MCRM was inverted with the selected maximum or minimum spectrum for a stand. All parameters were initially set free within specific intervals, some around values

given by Andres Kuusk (e-mail correspondence) and some self-estimated after some test modeling (see table 2). When the inversion could not produce a result, fixing one or a number of the parameters to specific values (see table 2), helped. Parameters resulting from the inversion were used to run MCRM in normal mode thereby producing a modeled reflectance spectrum. The modeled spectrum was visually compared with its respective measured spectrum. If good agreement was achieved, the inversion parameters were said to be acceptable for use in FRT. Otherwise, parameter adjustments were made in the inversion until the spectra showed good agreement.

***Table 2**: Intervals and fixed values for MCRM(inverted) parameters*

MCRM parameter	Values (A. Kuusk)	Interval
LAI	Non	Depending on amount of vegetation (not over 5)
Thm- Modal leaf angle	Non	0 – 90
Eln- leaf angle distribution	4.0	1 – 10
Sl- leaf size	0.2	0.1 – 0.5
Chlorophyll ($\mu g/cm^2$)	Non	0.1 – 50.0
Water (cm)	Non	0.001 – 0.030
Protein (g/cm^2)	Non	0.0001 – 0.0200
Cellulose + lignin (g/cm^2)	Non	0.001 – 0.03
N (# leaf layers)	Non	0.2 – 2.0
N_ratio	1.1	1.0 – 1.2
S1	Non	0.05 – 1.50
S2	Non	-0.5 – 1.5
S3	Non	-0.5 – 0.5
S4	Non	-1.0 – 0.5
Markov parameter	0.8	0.6 – 1.0

While FRT uses MCRM2 as a sub-model simulating a two layered ground vegetation structure, only one vegetation layer is modeled in MCRM. Thus, parameter data for one of the layers was not available. However, MCRM parameters can be used for one layer in MCRM2, if the other layer is made ”invisible” by setting the LAI and chlorophyll parameter values close to zero (LAI lower layer=0.001 and cAB=0.1) (Andres Kuusk, personal communication). Accordingly, MCRM parameters achieved

from inversion were used for the upper layer, while parameters for the lower layer were set to constant values in the FRT input files.

EWT, SLW and LAI values estimated from the field study of ground coverage were tested as in-parameters when inverting MCRM together with the respective ground reflectance spectrum. However, the model then could not produce any result. Because of this the values were not used and the model was inverted with parameter intervals and measured spectrums of ground reflectance as mentioned above.

6.2.3. PROSPECT inversion

For the PROSPECT inversion, mean value spectrums of one layered leaf or needle reflectance were calculated for each tree category from sun and shade reflectance spectrums measured with the ASD spectrometer in laboratory. The raw spectrum data were treated as the MCRM raw spectrums as mentioned in part 6.2.2 above. PROSPECT was inverted using the treated mean value spectrums together with the mean values of SLW and EWT, giving the values of cAB and N to be used in the FRT infile.

6.2.4. Calculation of FRT infile parameters

Parameters specifying the stand structure of the trees were mostly calculated from field and laboratory measurements. Values for aerosol and visibility data used by the 6S model were taken from the 6S simulation done for the Landsat TM scene over Scania (recorded 2000-06-10) used in Eklundh et al. (2003). This was done in order to reach similar atmospheric conditions as Eklundh, thereby making our reflectance conditions more comparable. The same sun zenith angle was used for all stands and was calculated for the coordinates 55 50 00 latitude, 13 25 00 longitude for date 2003-07-30, time 10:00 AM (+1h) using the ANGLES program. Occasionally, model default values and values from literature were used.

A typical stand input file for a single tree main class showing the parameters and how they were estimated is presented in Appendix 4.

6.3. Modeling FRT reflectance

FRT was run for all stand input files producing spectra of simulated stand reflectance. One spectrum representing maximum ground reflectance and one minimum was produced for each stand.

6.4. Statistical analysis

Values of stand reflectance representing maximum, minimum and mean ground reflectance (denoted TM/VI_{max} , TM/VI_{min}, TM/VI , where TM/VI = (TM/VI_{max} + TM/VI_{min}) divided by 2 (TM/VI is short for TM or VI)) were calculated for TM bands 1, 2, 3 and 4 and selected vegetation indices (see table 3). TM 5 and TM 7 were not calculated because the MCRM parameters only are representative for 400-1000 nm due to the limitations in optical range of the measured ground reflectance spectra (see 6.2.1 and 6.2.2.). Differences between TM/VI_{max} and TM/VI_{min} reflectance values (TM/VI_{max} - TM/VI_{min}) were also calculated (denoted TM/VI_{diff}).

A data set was constructed in which each stand had values of TM/VI_{max} , TM/VI_{min}, TM/VI, TM/VI_{diff}, the four vegetation indices, LAI estimates (L_e, L_{Gower}, L_{Chen}), modeled LAI ($LAI_{mod.}$ LAI_{ground}) and other stand parameters (e.g. stand density and crown radius).

***Table 3**: Vegetation indices (VI) used and how they where calculated. SR (Simple Ratio), NDVI (Normalized Difference Vegetation Index), ARVI (Atmospheric Reduction Vegetation Index) and SAVI (Soil Adjusted Vegetation Index).*

Index	Equation	Reference
SR	TM4 / TM3	Jordan, 1969
NDVI	TM4+TM3 / TM4-TM3	Rouse, 1974
SAVI	(1-L)(TM4-TM3 / TM4+TM3); L=0.5	Huete, 1988
ARVI	TM4-RB / TM4+RB; RB=TM3-γ(TM1-TM3); γ=1.0	Kaufmann and Tanré, 1992

The primary objective was to search out if and how much the ground reflectance affects the LAI values predicted by relationships between TM reflectance data and LAI estimates presented in Eklundh et al. (2003). Making this possible to calculate it was assumed that the stand reflectance simulated by FRT represented real TM reflectance for the stands and that they were comparable with the TM reflectance data presented in Eklundh et al. (2003). Thus, estimates and calculations made on FRT reflectance data were assumed to be applicable on Eklundh et al. (2003) reflectance data. In reality it is not totally correct to make such an assumption since the model describes an approximation of reality and Eklundh's data is real observed reflectance data.

Significant correlations were searched between the modeled TM/VI and TM/VI_{diff} for all tree categories. The regression equations from such significant correlations were applied on Eklundh et al. (2003) TM reflectance data to predict TM/VI_{diff} for these data (denoted $pred.TM/VI_{diff}$). The $pred.TM/VI_{diff}$ were added to and subtracted from each of the TM reflectance data to gain max and min reflectance data (denoted $ekl.TM/VI_{max}$, and $ekl.TM/VI_{min}$) that thus was said to be resulting from the difference in stand reflectance caused by ground reflectance for Eklundh et al. (2003) reflectance data.

LAI was then predicted for $ekl.TM/VI_{max}$ and $ekl.TM/VI_{min}$ using Eklundh et al., (2003) strongest regressions between TM reflectance and LAI_{Gower} (denoted LAI_{max} and LAI_{min}). These new LAI values were then plotted against. LAI was then predicted for the all the relationships using Eklundh's original TM reflectance data (denoted LAI_{org}). To visualize the effect that the variation in ground reflectance has on LAI calculated by the Eklundh´s (2003) linear empirical relationships LAI_{max} and LAI_{min} was plotted against LAI_{org}.

A regression analysis, using simple linear regression, was performed on the remaining dataset aiming at finding significant correlations between measured and modeled estimates of LAI and the vegetation indices, TM/VI_{mean}, and TM/VI_{diff} values.

Correlations between LAI estimates and various other stand parameters estimated by the model were also searched.

6.5. Sensitivity analysis

A sensitivity analysis of MCRM ground vegetation parameters was performed on stand L8 maximum and minimum reflectance. L8 was chosen because the MCRM parameters showed no unrealistic low or high values in comparison with the other stands. The chosen MCRM parameters were varied $\pm 25\%$, $\pm 50\%$, $\pm 75\%$, +100%, one at the time while keeping the others unchanged, thereby changing reflectance values of the FRT output reflectance spectra. The larger a change in reflectance when varying a parameter was, the more sensitive the model is to the parameter. The parameters used in the analysis were: Chlorophyll content (c_{AB}), water content (EWT), LAI, leaf structural parameter, leaf size parameter and specific leaf weight (SLW).

7. Results

7.1. Stand measurements and FRT parameters

Field measurements and ground cover observations resulted in a set of FRT parameters and various other data obtained for each stand, which in part can be viewed in table 4 below. A more complete list of the resulting data and the FRT parameters for each stand is presented in appendix 5.

Table 4: *Parameters for the stands measured in field (Le (effective LAI (PCA)), clumping factor (Ω) (TRAC), or calculated from variables measured in field (LAI Gower, LAI Chen, stand density(trees/m^2)), the stand tree type and mean values (mv) for the parameters (see also figure 4 Background).*

stand	tree type	Le (PCA)	LAI Gower	LAI Chen	stand density	clumping factor
L1	decidous	2.53	2.53	2.79	0.035	0.724
L2	decidous	3.12	3.12	2.93	0.077	0.871
L3	coniferous	3.92	5.10	5.78	0.047	0.794
L4	decidous	2.06	2.06	3.68	0.011	0.464
L5	decidous	3.04	3.04	2.73	0.028	0.875
L6	decidous	2.13	2.13	1.78	0.015	0.807
L7	coniferous	3.38	4.39	4.98	0.084	0.794
L8	coniferous	2.72	3.54	4.93	0.067	0.646
L9	coniferous	1.79	3.13	4.43	0.031	0.601
L10	decidous	3.91	3.91	2.99	0.018	0.999
L11	decidous	5.31	5.31	5.43	0.062	0.833
L12	decidous	5.17	5.17	5.21	0.061	0.828
L13	coniferous	2.01	3.52	3.67	0.037	0.816
L14	decidous	5.08	5.08	5.05	0.025	0.853
L15	decidous	3.60	3.60	3.77	0.025	0.770
L16	decidous	4.88	4.88	4.13	0.048	1.000
L17	decidous	4.65	4.65	4.07	0.052	0.963
L18	decidous	3.55	3.55	3.32	0.080	0.839
L19	coniferous	3.77	4.90	5.76	0.077	0.765
mv		**3.51**	**3.87**	**4.08**	**0.046**	**0.802**

7.1.1. MCRM parameters

The resulting parameters from the MCRM inversions used in the FRT input files are presented in appendix 6. It should be noted that they do not represent actual values of the ground vegetation and soil present in the stands, they represent the models best fit of parameters to represent the measured reflectance spectra.

7.1.2. PROSPECT parameters

Info about PROSPECT parameters used for modelling leaf reflectance in the FRT input files are presented in Emma Persson's degree thesis (unpublished).

7.2. FRT reflectance modelling

Mean value FRT reflectance resulting from simulations with MAX and MIN ground reflectance (TM/VI_{mean}) calculated for TM bands 1-4 for all stands are tabulated in appendix 7.

7.3. Statistical results

The modelling resulted in significant differences of TM band reflectance mean values due to variation in ground reflectance (TM/VI_{diff}) for several TM bands / VIs in each tree category. These values and the TM/VI means for each tree category are tabulated below (table 5) together with the percentage TM/VI_{diff} of TM/VI.

Table 5: *Mean values (mv) for the modelled TM-data and vegetation index (SR, NDVI, ARVI, SAVI), for the means of the difference in modelled reflectance due to the influence of ground reflectance (mvdiff), and mvdiff presented as percent of mv. The stars (*) are showing the level of significance (*=p<0.15 and **=p<0.05) for the mean TM-data difference due to ground reflectance. Coniferous=con. , deciduous=dec..*

ALL (n=19)	**TM 1**	**TM 2**	**TM 3**	**TM 4**	**SR**	**NDVI**	**ARVI**	**SAVI**
mv	0.0297	0.0579	0.0355	0.2642	7.999	0.761	0.728	0.427
mv diff	-0.0003	0.0015	-0.0035	0.0407	1.974	0.056	0.078	0.062
mvdiff % of mv	**-0.9**	**2.5**	**-9.8**	**15.4**	**24.7**	**7.3**	**10.7**	**14.6**
mvdiff sign.			**	**	**	**	**	**
DEC. (n=13)	**TM 1**	**TM 2**	**TM 3**	**TM 4**	**SR**	**NDVI**	**ARVI**	**SAVI**
mv	0.0322	0.0619	0.0387	0.2715	7.576	0.748	0.712	0.429
mv diff	0.0006	0.0030	-0.0029	0.0460	1.875	0.056	0.080	0.067
mvdiff % of mv	**1.8**	**4.8**	**-7.5**	**16.9**	**24.8**	**7.5**	**11.2**	**15.6**
mvdiff sign.		**	*	**	**	**	**	**
CON. (n=6)	**TM 1**	**TM 2**	**TM 3**	**TM 4**	**SR**	**NDVI**	**ARVI**	**SAVI**
mv	0.0244	0.0493	0.0286	0.2482	8.917	0.790	0.763	0.423
mv diff	-0.0021	-0.0018	-0.0047	0.0292	2.187	0.055	0.074	0.052
mvdiff % of mv	**-8.5**	**-3.7**	**-16.5**	**11.8**	**24.5**	**7.0**	**9.7**	**12.3**
mvdiff sign.			*	*	**	**	**	**

The reflectance is over-all slightly higher for the deciduous (dec.) stands than for coniferous (con.). The mean value differences (mvdiff) are following the general

pattern for vegetation of being positive in reflective areas and negative in absorptive areas for all the significant values. The variation in ground reflectance (mvdiff) makes up about 24% of SR for all categories followed in size by SAVI and TM3 and TM4.

Two significant negative correlations were found for the coniferous category between values of modelled VI (NDVI, ARVI) and difference in modelled VI (NDVI diff., ARVI diff.) resulting from variation in measured ground reflectance (see figure 7a-b below). The regressions have probability and correlation values of p=0.033, r=0.8477 for NDVI, and p=0.015, r=0.897 for ARVI as calculated by an ANOVA.

a)

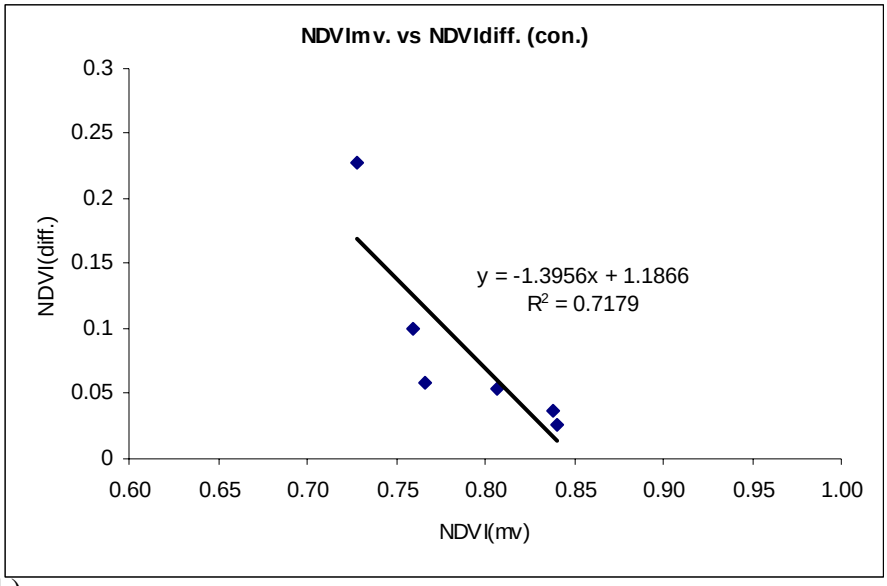

b)

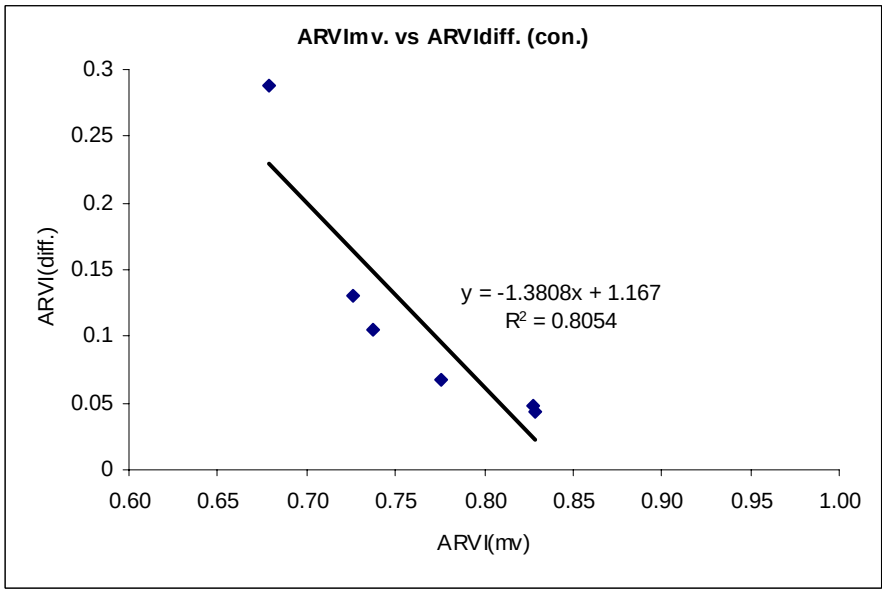

Figure 7a-b: *Regressions between modelled VI (a:NDVI and b:ARVI) and modelled differences in the respective VI due to ground reflectance (NDVIdiff. and ARVIdiff.).*

The regressions (figure 7a-b) are used to predict $VI_{diff.}$ for Eklundh et al.,(2003) ARVI and NDVI data (denoted pred.$ARVI_{diff}$ and pred.$NDVI_{diff}$).). The pred.TM/VI_{diff} are added to and subtracted from each of Eklundh's ARVI and NDVI data for coniferous stands to gain max and min reflectance data that is said to be resulting from the difference in stand reflectance caused by ground reflectance for Eklundh et al.(2003) reflectance data (denoted Ekl.VI_{max}, and Ekl.VI_{min}). LAI is predicted for these data as well as for Eklundh's original ARVI and NDVI data using Eklundh et al.,(2003) LAI vs TM-data regressions for NDVI and ARVI. LAI predicted from the Ekl.VI_{max} and Ekl.VI_{min} plotted against LAI predicted from Eklundh's original VI data is presented in figure 8a-b. As seen, there is dramatic difference in predicted LAI, especially for lower LAI, depending on the variation of measured ground reflectance.

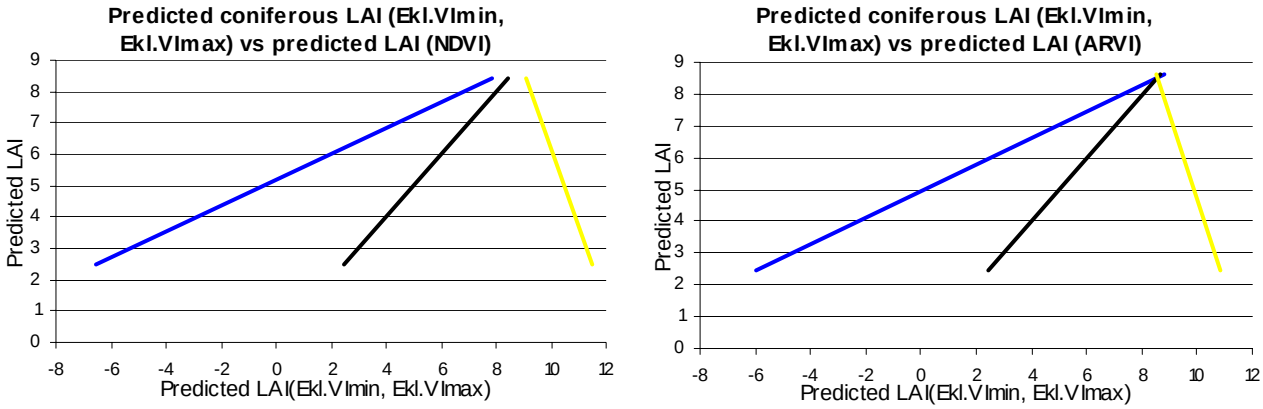

Figure 8a-b: *Predicted coniferouos LAI according to Eklundh,(2003) LAI vs VI regressions for NDVI (a) and ARVI(b) using EklVI_{min} (blue), Ekl.VI_{max} (yellow) and Eklundh's original VI (black) values. The data is plotted against LAI predicted according to Eklundh,et al.,(2003) original LAI vs VI regressions for NDVI and ARVI. The blue regression line is when LAI is predicted with the variation in ground reflectance subtracted, the yellow when the variation is added. Only the regression lines are shown since all of the three relationships only differ in sloping coefficients.*

Modelled reflectance data and measured LAI compared to Eklundh et al. (2003) reflectance and LAI data are presented in figure 9a-g below.

a)

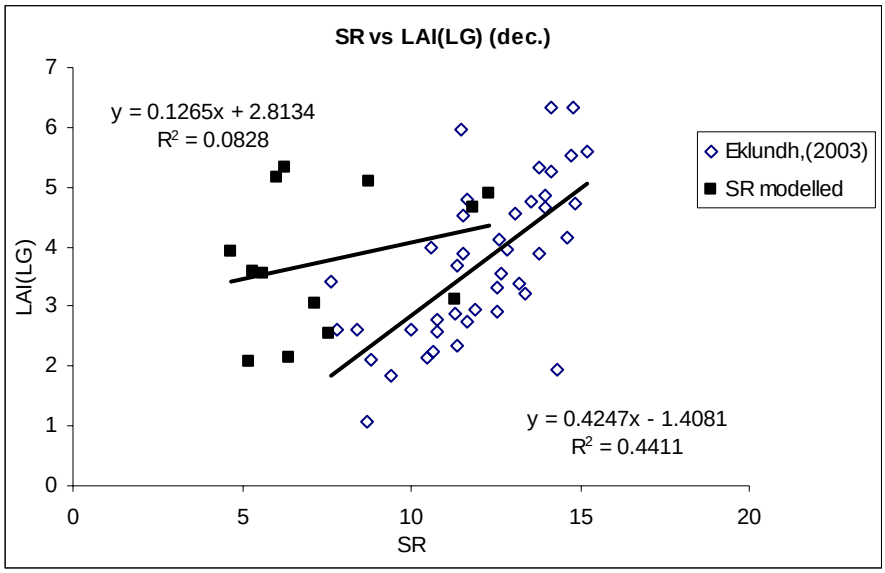

b)

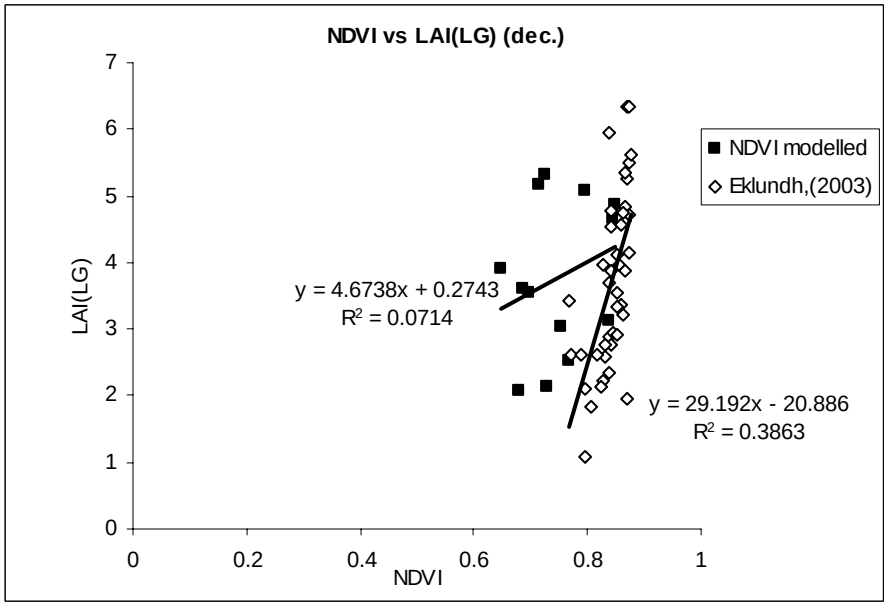

c)

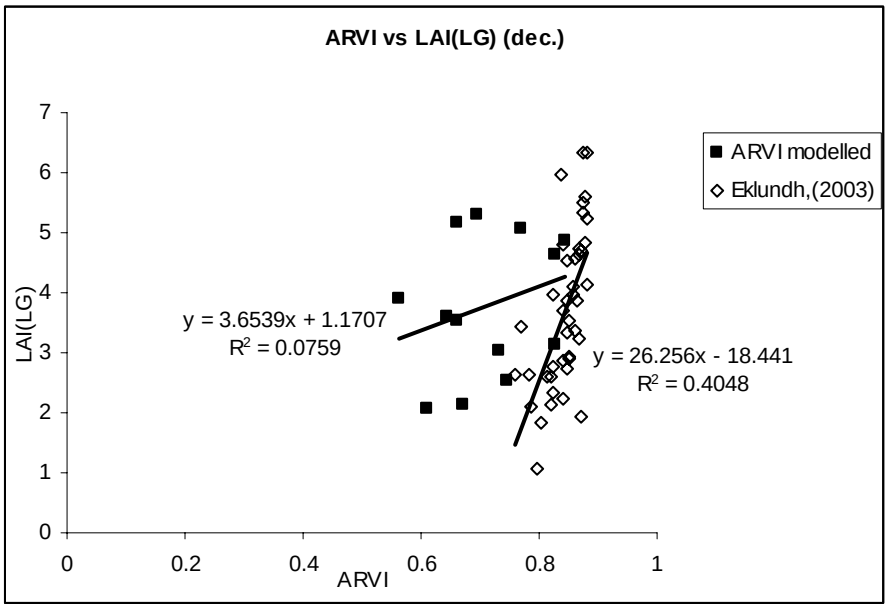
ARVI vs LAI(LG) (dec.)
ARVI modelled
Eklundh,(2003)
y = 3.6539x + 1.1707
R2 = 0.0759
y = 26.256x - 18.441
R2 = 0.4048
LAI(LG)
ARVI
0
1
2
3
4
5
6
7
0
0.2
0.4
0.6
0.8
1

d)

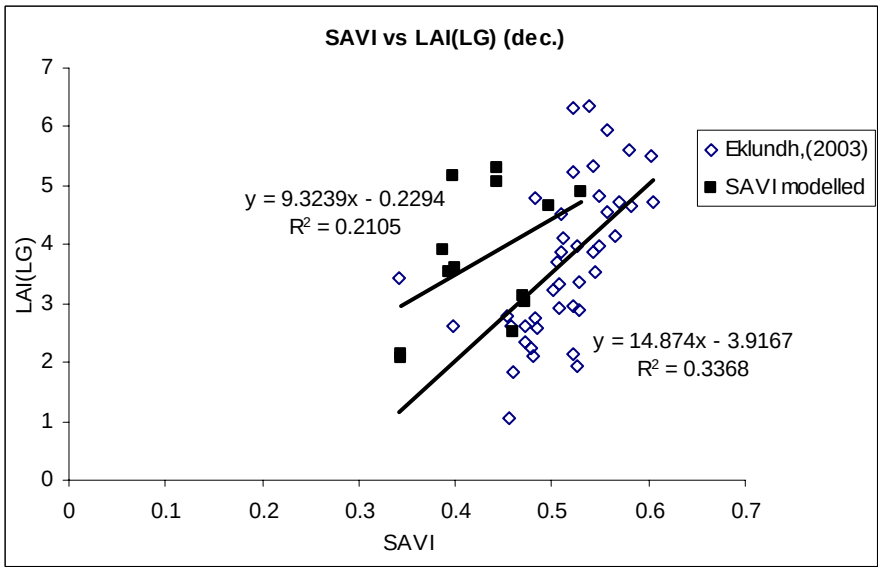
SAVI vs LAI(LG) (dec.)
Eklundh,(2003)
SAVI modelled
y = 9.3239x - 0.2294
R2 = 0.2105
y = 14.874x - 3.9167
R2 = 0.3368
LAI(LG)
SAVI
0
1
2
3
4
5
6
7
0
0.1
0.2
0.3
0.4
0.5
0.6
0.7

e)

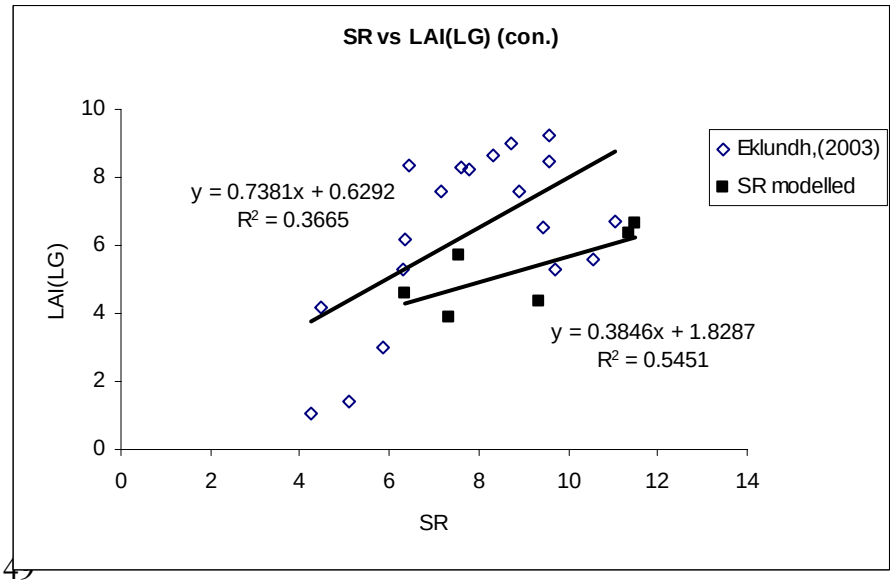
SR vs LAI(LG) (con.)
Eklundh,(2003)
SR modelled
y = 0.7381x + 0.6292
R2 = 0.3665
y = 0.3846x + 1.8287
R2 = 0.5451
LAI(LG)
SR
0
2
4
6
8
10
0
2
4
6
8
10
12
14

f)

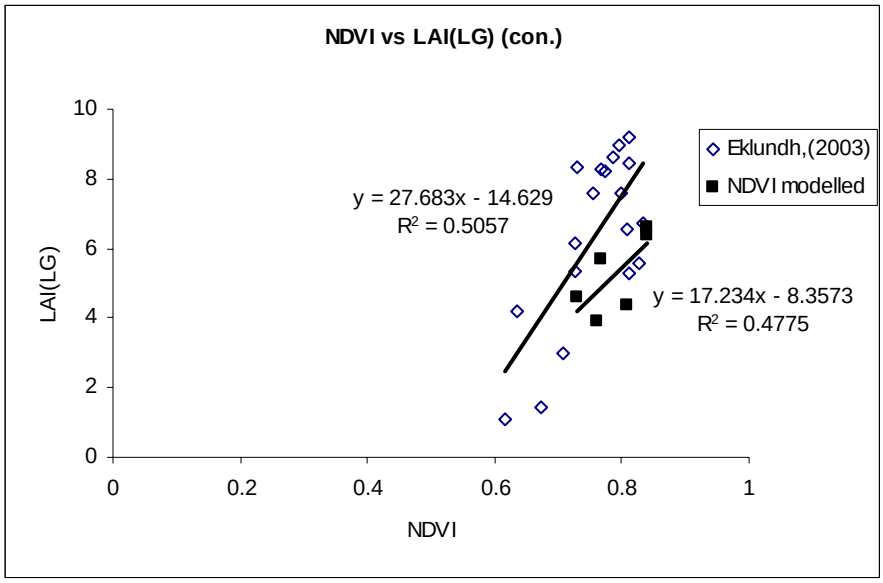

g)

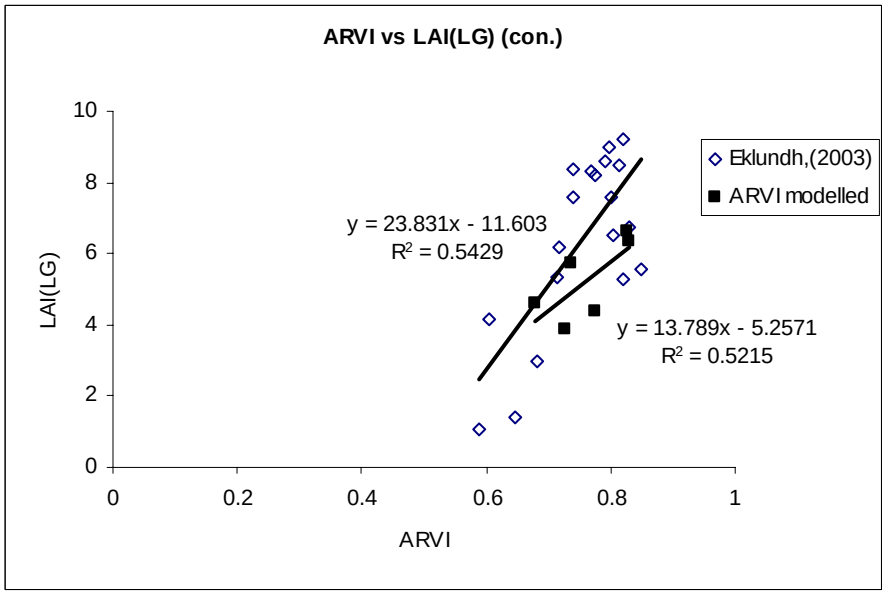

***Figure 9a-g**: Comparison of modelled TM reflectance and Eklundh et al.,(2003) TM reflectance plotted against LAI(L_{Gower}) for a) SR dec. b) NDVI dec. c) ARVI dec. d) SAVI dec. e) SR con. f) NDVI con. g) ARVI con.. Presented with linear regressions and r^2-values.*

In general there are small similarities between the two datasets. The closest matches are for NDVI (figure 9b) and SAVI (figure 9d) for the deciduous category. Modelled SAVI is best correlated to LAI_{Gower} for the deciduous category (r = 0.46, non significant) and SR is best for coniferous (r = 0.77, significant p= 0.071). There are generally higher correlations for the coniferous stands.

The regression analysis made between LAIs calculated from field measurements (Le, L_{Gower}, L_{Chen}) and modelled parameters of FRT and the MCRM2 sub model of ground reflectance resulted in plots with significant correlations presented in Figure 10a-d and Table 6 below.

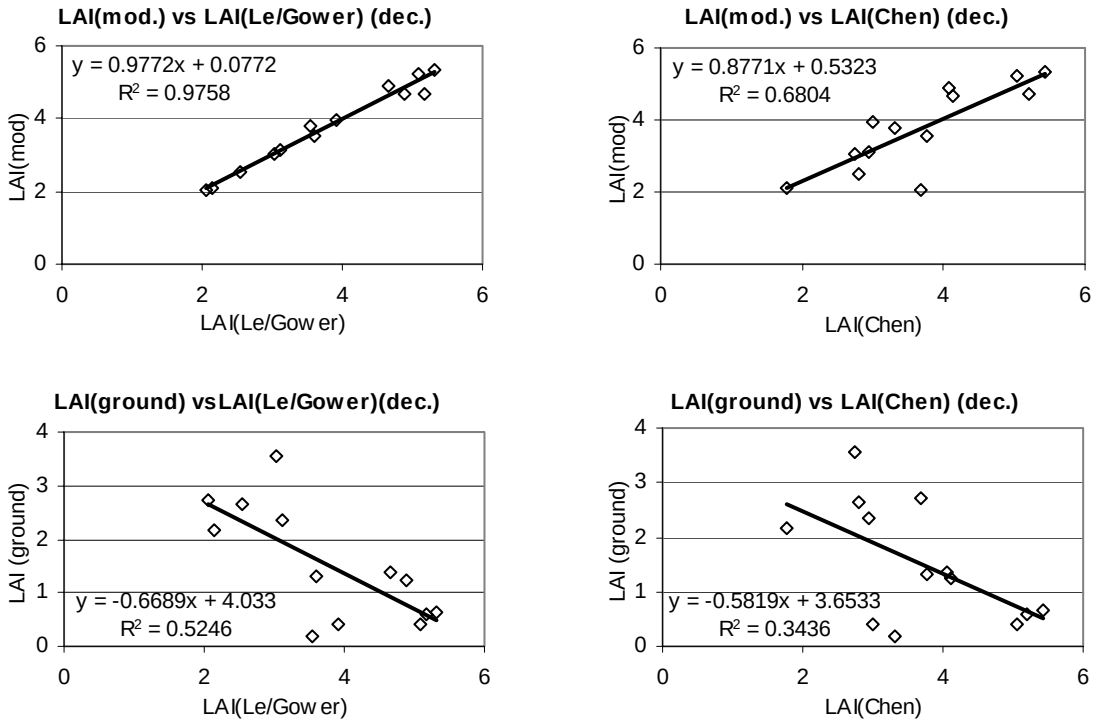

***Figure 10a-d**: Modeled LAI versus LAI calculated from field measurements (LAI(Gower), LAI(Chen)) is presented in figure a and b. Modeled ground LAI versus LAI calculated from field measurements (LAI(Gower), LAI(Chen)) is presented in figure c and d. All plots are for the deciduous stands and are presented with regression equation and r^2-value.*

***Table 6**: Relationships between modeled LAI and ground LAI versus LAI calculated from field measurements (LAI(Le), LAI(Gower), LAI(Chen)) for all tree categories presented together with r, r^2 and p-values.*

type	relationship	r	r square	p-value
ALL	LAI(mod.) vs Le	0.97	0.94	inf.
	LAI(mod.) vs LG	0.81	0.66	inf.
	LAI(mod.) vs LC	0.42	0.17	0.077
DEC.	LAI(mod.) vs LG	0.99	0.98	inf.
	LAI(mod.) vs LC	0.82	0.68	0.001
CON.	LAI(mod.) vs Le	0.91	0.82	0.013
	LAI(mod.) vs LG	0.96	0.93	0.002
	LAI(mod.) vs LC	0.85	0.73	0.031
ALL	LAI(ground) vs Le	-0.70	0.49	0.001
	LAI(ground) vs LG	-0.69	0.47	0.001
	LAI(ground) vs LC	-0.46	0.21	0.046
DEC.	LAI(ground) vs LG	-0.72	0.52	0.005
	LAI(ground) vs LC	-0.59	0.34	0.035
CON.	LAI(ground) vs Le	-0.81	0.66	0.050
	LAI(ground) vs LG	-0.66	0.44	0.150
	LAI(ground) vs LC	-0.71	0.50	0.116

It is interesting to note that the modelled LAI in general is best correlated with LAI_{Gower} even though LAI_{Chen} is used as in-data. This is also true for LAI(ground) except for the coniferous category where LAI_{Chen} has somewhat higher correlation.

7.4. Sensitivity analysis

The sensitivity analysis made on L8 MAX and L8 MIN resulted in values of forest reflectance for each sensitivity level per parameter that had been varied. The reflectance values were plotted against their respective wavelength giving a set of graphs for each sensitivity level per varied parameter. The graphs for L8 MAX are presented in Figure 11a-f and the graphs for L8 MIN are presented in Figure 12a-f.

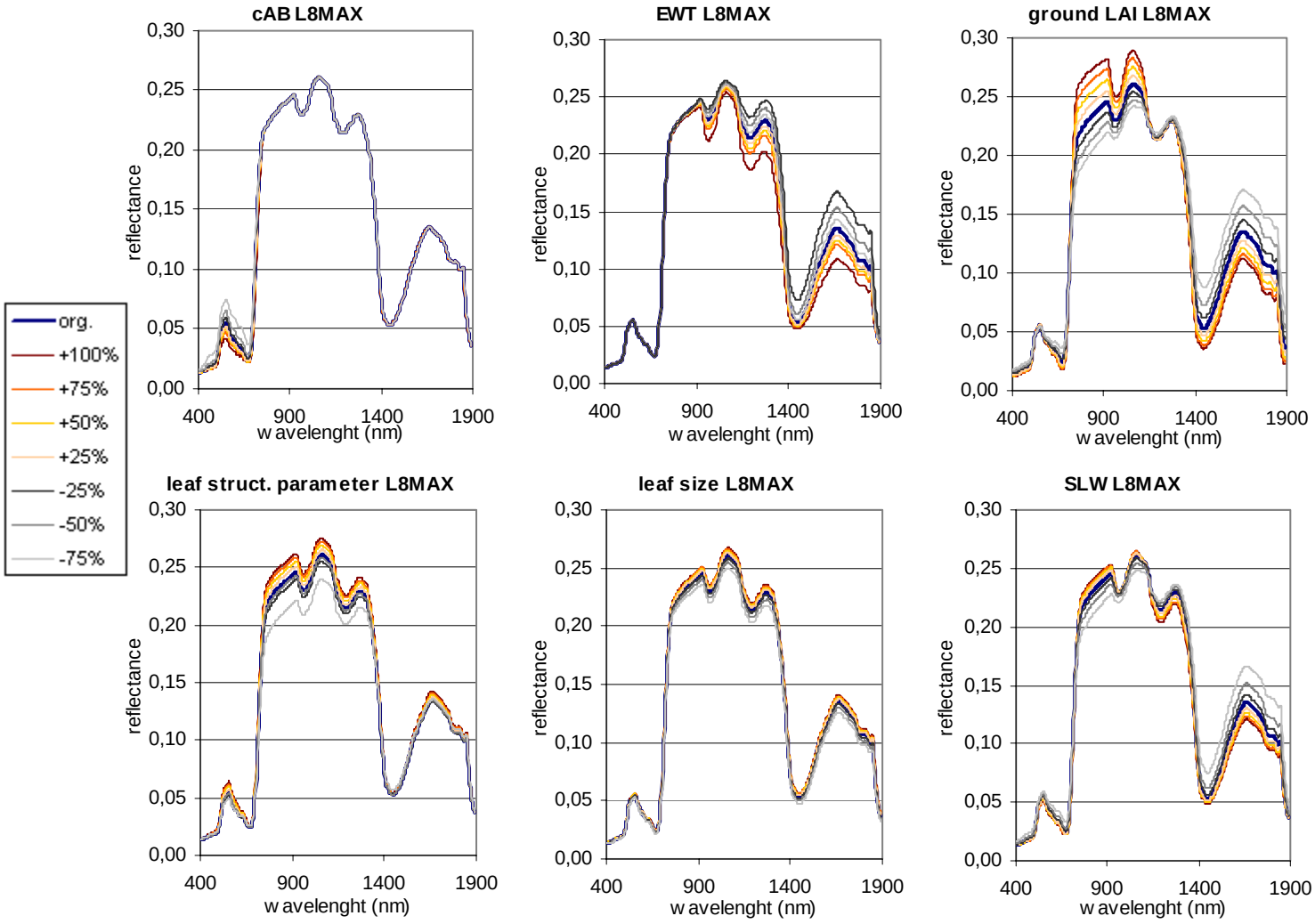

***Figure 11a-f**: Sensitivity diagrams resulting from the sensitivity analysis made on L8 MAX.*

Parameters showing large impact throughout the simulated reflectance spectrum for L8 MAX are in descending order: ground LAI, SLW and the leaf structural parameter. EWT has large impact from 900 – 1900nm and cAB impact in the visible part of the spectrum (400 – 700nm) whereas leaf size has impact in about 800 – 1900nm.

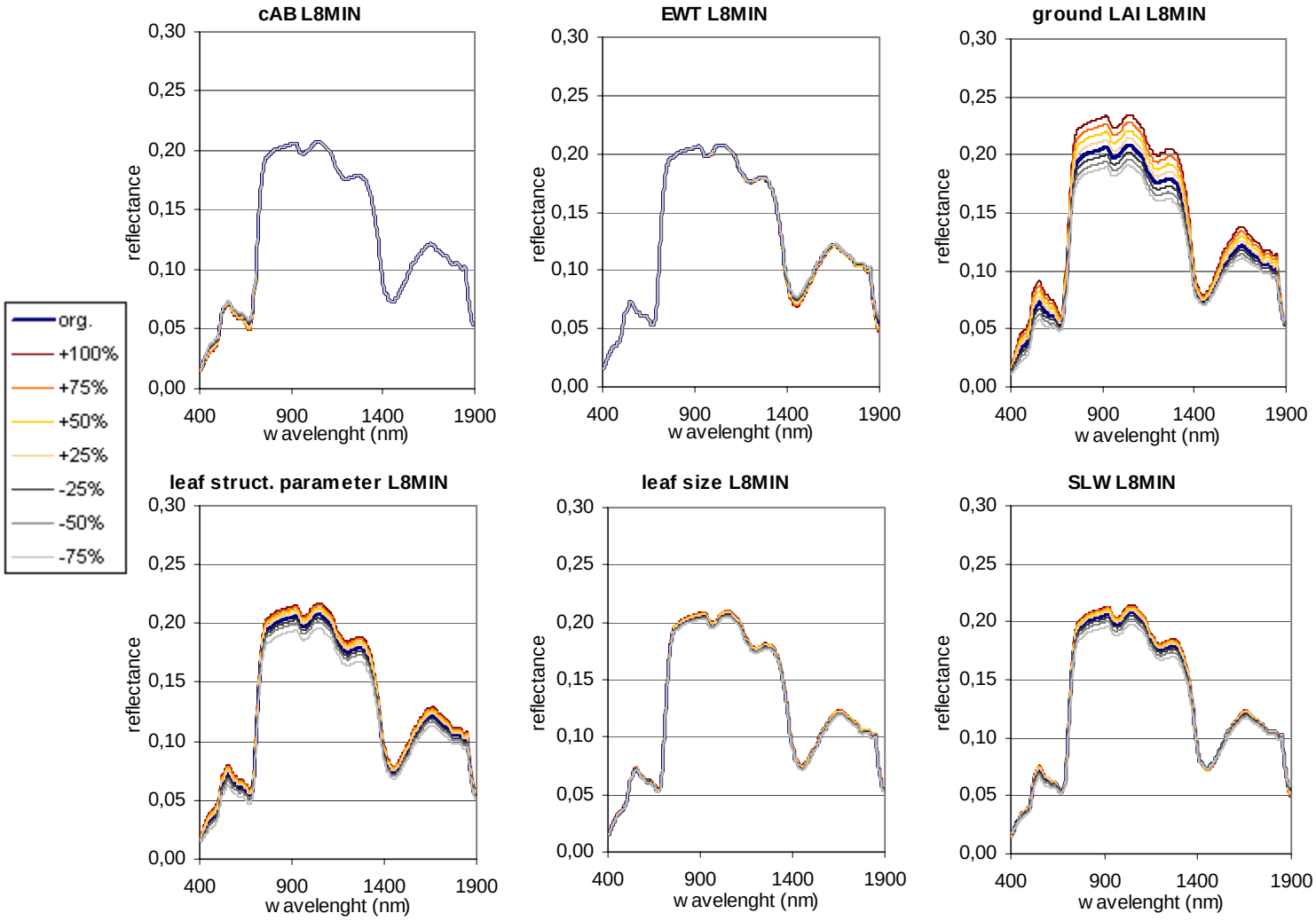

***Figure 12a-f**: Sensitivity diagrams resulting from the sensitivity analysis made on L8 MIN.*

In the L8 MIN sensitivity simulations ground LAI has a clearly dominating impact on reflectance throughout spectrum followed in importance by the leaf structural parameter. SLW has impact in about 800 – 1300nm whereas the other three show to have minor importance or non at all.

8. Discussion

Reflectance of the forest floor (ground reflectance) contributes to forest reflectance in varying degree throughout the optical spectral range due to the absorption features of green vegetation, dead tree/plant material and soil. Various authors (Spanner et al., 1990; Chen, 1996; Chen and Cihlar, 1996; Eklundh et al., 2001) have stressed the importance of better understanding the effects of ground reflectance in forest reflectance produced by reflectance models and measured by satellites. The results of this study (table 5b) show significant difference in forest reflectance due to ground reflectance for TM 3, TM 4 and all the studied VI's for deciduous, coniferous and combined as well as for TM 2 for the deciduous. It can thereby be concluded that ground reflectance should have a significant influence on forest reflectance measured by satellites and estimated by reflectance models (if forest reflectance is assumed to be reflectance constituted by the trees in the forest only). However, the magnitude of this influence is affected by uncertainties involved at different steps in the process of their estimation.

Since the study has a modelling approach it is vital to focus on discuss some uncertainties around the reflectance models used. FRT uses the spectral reflectance and transmittance data calculated by PROSPECT2 as input. The FRT algorithm then acts on these spectral data taking all of the other stated stand parameters into consideration. Following this, as is stated in Kuusk and Nilson (2000), the spectral properties and therefore the performance of FRT are greatly determined by the accuracy of the PROSPECT2 model. This is also the case with the MCRM2 and MCRM models since they also use the PROSPECT2 model in a similar manner. The NIR-region has been stated as FRTs most problematic region when modelling forest reflectance since there is a clear underestimation of absorption in this part of the spectrum; this is especially evident for deciduous forests (Kuusk and Nilson, 2000). This may be due to unaccountancy of some mechanism of NIR absorption in the model algorithm or due to underestimation of NIR absorption by the PROSPECT2 model (ibid.). PROSPECT2 is known to have problems modelling in the 780 – 920nm (NIR) part of the spectrum due to that absorption coefficients of biophysical parameters and the structural parameter (N) representing the absorption features in this region are correlated (Jacquemoud and Barret, 1990; Jacquemoud et al., 1996).

When MCRM was inverted with the reflectance spectrums a set of parameter intervals was used and not data from field measurements since the model could not produce result when these were used. The resulting set of MCRM parameter values therefore may inhabit large errors in respect of representing actual biophysical values. However, the parameters represent a close fit to the measured spectra so when the values are used to simulate ground reflectance in FRT they do it satisfactory.

Parameters representing the physical structure of the forest stands in FRT are based on measurements of only 3 to 4 trees for the main species tree size class and 1 to 2 trees for the sub-species. It is therefore questionable whether the parameters are in fact representative for the stand structure since the trees in the stands are heterogeneous, more so in deciduous stands than in coniferous. More trees should be measured in order to achieve better representation of the stand structure in FRT.

The ground reflectance spectrums measured by the spectrometer contain in themselves potential sources of error. There was often a variation in above-canopy light conditions due to difference in sun angles and cloud cover between the individual measurements in a stand and even more so between measurements in different stands. This is because the measurements were made over a three-month period at different geographic places and time of day. The differences in the proportions of direct and diffuse radiation that thereby follows affects the spectrum configuration being much more noisy in sunny weather conditions than in cloudy. The comparability between the spectrums may thereby be affected which ultimately may lead to that the reliability of the estimates of the TM reflectance differences due to variation in ground reflectance is lessened.

Two significant negative linear relationships were found for the coniferous category (n=6) between NDVI and ARVI and the difference in these VI's due to variation in ground reflectance ($NDVI_{diff}$ and $ARVI_{diff}$) (figure 7a-b). No relationship were found to be significant for deciduous (n=13) or for deciduous and coniferous combined. The significant relationships for conifers imply that the VI part reflected by the forest floor (ground reflectance) is increasing as forest VI as whole is decreasing. When calculating new VI for Eklundh's data using the regression equations from the

relationships of $NDVI_{diff}$ vs NDVI and $ARVI_{diff}$ vs ARVI and predict LAI with Eklundh's LAI vs VI relationships it was found that the variation in ground reflectance has a huge impact on predicted LAI (figure 8a-b). The effect is especially pronounced for lower LAI. However, the size of the effect is to be interpreted carefully since the VI_{diff} is both added and subtracted. It should probably only be subtracted since ground vegetation is an additive effect in VI vs LAI relationships (i.e. the ground VI has positive values and thus increases the forest VI). The size of the effect can partially be explained by the high sloping coefficients of Eklundh's relationships used to predict LAI. This makes the relationships sensitive for manipulation of the VI values because even a smaller change in VI would generate a big difference in predicted LAI. If the coefficients of the relationships were lower the effect of ground reflectance would be lessened. There is good agreement between my modelled VI data and Eklundh's for conifers, (figure 9f-g) since the sloping coefficients are similar for the relationships of LAI vs NDVI and ARVI. Because of the similarity there could be reasons to assume that the ground VI predicted by my relationships of $NDVI_{diff}$ vs NDVI and $ARVI_{diff}$ vs ARVI are realistic estimates for the real situation in scanian coniferous forests and further, that their effect on predicted LAI using Eklundh's relationships also is realistic. To reach the similarity between Eklundh's and my data LAI_{Gower} had to be recalculated in the same manner as Eklundh's by altering the γ for pine to 2.17 and for spruce to 1.69. The strength of my relationships was then somewhat lessened as was the p-values, but higher similarity between the datasets was achieved.

No significant relationships were found for deciduous forest either for VI_{diff} vs VI or LAI_{Gower} vs VI, even though the higher number of observations (figure 9a-d). Research has often focused on boreal conifers when it comes to forest LAI and reflectance studies and little attention has been diverted to deciduous forests. The reason for lack of positive results for deciduous forest could be modelling aspects and the presence of stands with different species, each having unique spectral characteristics. But even when beech (n=9) solely was studied there were only weak relationships. It could be that the model has some trouble related to describing the deciduous canopy structure, which is much less structured than that of conifers. Other aspects to consider is the variability in ground vegetation in the stands, the stand

productivity (swe. bonitet) and amount of ground water and how these two latter factors affect the amount of ground vegetation present in the stands. Presence or absence of ground vegetation greatly affects the configuration of a measured ground reflectance spectrum. The ground of the beech forest studied was mostly covered with dead leaves with occasional patches of ground vegetation, conditions giving a high variation in ground reflectance. In the coniferous forest mostly green mosses were present with patches of dead twigs and needles, giving a lower variation in ground reflectance. The higher variation in ground reflectance in the deciduous stands could perhaps explain the absence of relationships in VI_{diff} vs VI for the deciduous stands.

In the sensitivity analysis of L8 max and min (figure 11 a-f , 12 a-f), ground LAI was shown to be the most important parameter controlling ground reflectance and showed high sensitivity over the whole modelled spectrum (400-1900 nm). The result is congruent with Kuusk (2004), which also states ground LAI as the primary driving parameter of ground reflectance for MCRM. The leaf structural parameter, leaf weight (SLW) and leaf size are of descending sensitivity also active throughout the whole spectrum but weaker than ground LAI. Leaf water (EWT) and chlorophyll content (cAB) are active in their respective absorptive areas of the spectrum. Reasons for the differing response patterns between L8 max and min are to a large degree explained by the original parameter values, being considerably lower for L8 min. Changing a parameter + or -100% will not make much difference to the resulting reflectance when starting from a low value but it will lead to considerable effects starting from higher values. L8 min will due to a low value of ground LAI also have more response from soil (which parameters are not considered in the sensitivity analysis and which also differs in importance between L8 max and min).

L_{Gower} was strongest correlated to modelled LAI for both the deciduous and coniferous categories separately (figure 10 a-d, table 6). Taken together L_e gives the strongest correlation whereas L_{Gower} is weaker, which could suggest that L_e has an ability to merge the two categories representing an estimate of LAI. L_{Chen} is weakest correlated to modelled LAI for all categories. It is surprising since the L_{Chen} estimate was considered as the closest estimate to real LAI in this study because it compensates for both presence of woody material and clumping of vegetation elements on shoot and canopy level. It is even more surprising since L_{Chen} is used

when calculating the in-data estimate of total leaf weight/tree when modelling with FRT. Reasons for the contradictory result is unknown but considering the other in-parameters measured in field these could suggest a structure of the canopy in the stands that more closely assembles the LAI response of L_{Gower}. Other suggestions are that L_{Chen} is a reliable estimate of real LAI but that FRT is unable to estimate real LAI or that some of the related model parameter calculations are faulty in some way.

It is interesting to have found relatively strong statistically significant negative relationships between modelled ground LAI and the LAI estimates (table 6). The strongest relationship was found between LAI ground and L_e for conifers (r^2=0,66 (table 6)). This data confirms theory that the lower forest LAI the higher transmittance to the forest floor and subsequently the higher ground LAI. Such relationships also make it possible to predict the ground LAI in LAI calculated from forest satellite reflectance as Eriksson et al. (2006) also concludes. It also confirms the usefulness of forest reflectance models for such applications. L_e is the best predictor of ground LAI, possibly since L_e is a parameter that is related to radiation interception of PAR through the canopy and not actual LAI (Chen and Cihlar, 1996, Li-Cor. Inc., 1992). The levels of PAR on the forest floor greatly determine the amount of ground vegetation present.

The results of my study point towards that forest LAI predicted by empirical relationships between satellite reflectance and LAI estimates are seriously affected by ground reflectance. The LAI values should be used with caution as in-data when modelling (f.e.GCMs, carbon cycling). Satellite data could also be affected by various other factors such as variation in sun elevation (satellite data registration), canopy structure, atmospheric conditions and more besides being affected by the variation in ground reflectance, but their effects are not investigated in this project. For future investigations considering ground reflectance I suggest focus on producing reliable relationships between satellite reflectance and variation in ground reflectance with help of a reflectance model such as FRT. These relationships could then be used to correct satellite data for ground reflectance, data that in turn can be related to ground measured estimates of forest LAI, hopefully achieving stronger relationships that can predict forest LAI from satellite data more accurately.

9. Conclusions

Significant negative linear relationships were observed for the coniferous stands between the vegetation indexes ARVI and NDVI and the response of these due to simulation the variation in ground reflectance. No significant relationship was found for the deciduous category. However, significant mean values of differences in modelled VI and TM reflectance were observed for both of the forest types. The results point towards that ground reflectance has a significant impact on forest canopy reflectance that seriously could decrease the accuracy of LAI predicted by empirical relationships of satellite reflectance. I suggest correction of the satellite reflectance for ground reflectance in order to achieve more reliable LAI estimates for sub- boreal and boreal forests.

Significant negative relationships were found between forest LAI estimates and modelled LAI of the ground vegetation for all the forest stands (r^2=0.49). The relationships were stronger when deciduous and coniferous stands were separated. Thus, ground LAI can be predicted from LAI values of the forest canopy relatively satisfactory.

Significant linear relationships were observed between canopy LAI and the vegetation index SR, NDVI and ARVI for the coniferous stands. There were no significant relationships observed for the deciduous stands. There is good agreement between the conifer relationships and existing relationships from the measurement area (found in Eklundh et al., 2003), which suggests that FRT models coniferous stands satisfactory. This could not be said for deciduous forest, which probably needs more modelling consideration.

Inversion of ground reflectance spectra in MCRM with the given parameter intervals (table 2, section 6.2.2.) seems promising for retrieving parameters representing ground reflectance to be used in FRT and to predict values of ground LAI. Using ground reflectance spectra covering the whole of the modelled spectrum (400-2600nm) could improve the results.

The sensitivity analysis of parameters of ground vegetation in FRT shows the ground LAI parameter to be the most sensible. An increased sensitivity of all ground vegetation parameters was observed the more vegetation was present.

Over all, the results of this study show that ground reflectance needs to be taken into consideration, and compensated for when estimating forest LAI from satellite reflectance using empirical linear relationships. LAI values predicted from satellite data not compensated for ground reflectance should be used with caution in models (f.e.GCMs, carbon cycling) when representing amount of vegetation.

10. References

Black, T.A., Chen, J.M., Lee, X., Sagar, R.M., 1991. Characteristics of shortwave and longwave irradiances under a Douglas-fir forest stand. Canadian Journal of Forest Research 21, 1020–1028.

Barrett, E.C. and Curtis, L.F.: Introduction to environmental remote sensing. Chapman and Hall, London, 1976.

Campbell, J. B. (1996). "Introduction to Remote Sensing", Taylor & Francis Ltd.

Chen, J. M. (1996). Optically-based methods for measuring seasonal variation of leaf area index in boreal conifer stands. Agricultural and Forest Meteorology, 80, 135−163.

Chen, J. M., & Black, T. A. (1992). Defining leaf area index for non-flat leaves. Plant Cell and Environment, 15, 421−429.

Chen, J. M., & Cihlar, J. (1995). Plant canopy gap size analysis theory for improving optical measurements of leaf area index. Applied Optics, 34, 6211−6222.

Chen, J. M., & Cihlar, J. (1996). Retrieving leaf area index of boreal conifer forests using Landsat TM images. Remote Sensing of Environment, 55, 153−162.

Cutini A, Matteucci G, Mugnozza GS (1998) Estimation of leaf area index with the Li-Cor LAI-2000 in deciduous forests. Forest Ecological Management 105:55–65

Danson, F.M. and Curran, P.J. 1993. Factors affecting the remotely sensed response of coniferous forest plantations. Remote Sensing of Environment. 43: 55-65.

Disney, M.I.(2002): Improved estimation of surface biophysical parameters through inversion of linear BRDF models.
http://www.geog.ucl.ac.uk/~mdisney/phd.bak/final_version/final_pdf/cover.pdf

Eklundh, L., Hall, K., Eriksson, H., Ardö, J., & Pilesjö, P. (2003). Investigating the use of Landsat thematic mapper data for estimation of forest leaf area index in southern Sweden. Canadian Journal of Remote Sensing, 29, 349−362.

Eklundh, L., Harrie, L., & Kuusk, A. (2001). Investigating relationships between Landsat ETM+ sensor data and leaf area index in a boreal conifer forest. Remote Sensing of Environment, 78, 239−251.

Eriksson, H.M., Eklundh, L., Kuusk, A., and Nilson, T. (2006) Impact of understory vegetation on forest canopy reflectance and remotely sensed LAI estimates. Remote Sensing of Environment 103(4), 408-418.

Eriksson, H., Eklundh, L., & Lindroth, A. (2005). Estimating LAI in deciduous forests. Agricultural and Forest Meteorology, 129, 27−37.

Gao, X., Huete, A.R., NiW., and Miura, T., 2000, Optical-biophysical relationships of vegetation spectra without background contamination, Remote Sensing of Environment, 74:609-620.

Goel N. S., 1989. Inversion of Canopy Reflectance Models for Estimation of Biophysical Parameters from Reflectance Data, in Theory and Applications of Optical Remote Sensing (Asrar G., Ed.). John Wiley & Sons.

Gower, S. T., Kucharik, C. J., & Norman, J. M. (1999). Direct and indirect estimation of leaf area index, fAPAR, and net primary production of terrestrial ecosystems. Remote Sensing of Environment, 70, 29−51.

Gower ST and Norman JM (1991): Rapid estimation of leaf area index in conifer and broad-leaf plantations. Ecology 72(5): 1896-1900.

Huete, A.R. (1988): A soil-adjusted vegetation index (SAVI). Remote Sensing of Environment, v.25, p.295-309.

Jacquemoud, S., & Baret, F. (1990). PROSPECT: A model of leaf optical properties spectra. Remote Sensing of Environment, 34, 75−90.

Jacquemoud, S., Ustin, L., Verdebout, J., Schmuck, G., Andreoli, G. and Hosgood, B. (1996). "Estimating Leaf Biochemistry Using the PROSPECT Leaf Optical Model". Remote Sensing of Environment, 56:194-202.

Jordan, C.F. (1969): Derivation of leaf-area index from quality of light on the forest floor. Ecology, v.50, p.663-666.

Kaufman, Y. J. (1989). "The Atmospheric Effect on Remote Sensing and its Correction" in Theory and Applications of Optical Remote Sensing (Asrar, G., Ed), John Wiley & Sons.

Kaufman, Y.J. and Tanré, D., 1992, Atmospherically resistant vegetation index (ARVI) for EOS-MODIS, IEEE Transactions on Geoscience and Remote Sensing, 30:261-270.

Kuusk, A. and Nilson, T.(2002): Forest Reflectance and Transmittance FRT User Guide. www.aai.ee/bgf/frt/ (link to the most recent version of FRT)

Kuusk, A. (2001). A two-layer canopy reflectance model. Journal of Quantitative Spectroscopy & Radiative Transfer, 71(1), 1−9.

Kuusk, A., Lang, M., & Nilson, T. (2004). Simulation of the reflectance of ground vegetation in sub-boreal forests. Agricultural and Forest Meteorology, 126, 33−46.

Kuusk, A., & Nilson, T. (2000). A directional multispectral forest reflectance model. Remote Sensing of Environment, 72, 244−252.

Kuusk, A. (1995) A Markov chain model of canopy reflectance, Agricultural and Forest Meteorology, 76(3-4), 221-236.

Law, B.E. and R.H. Waring (1994) Combining remote-sensing and climatic data to estimate net primary production across Oregon. Ecological Applications 4, 717-728.

Leblanc, S. G. (2002):Correction to the plant canopy gap size analysis theory used by the Tracing Radiation and Architecture of Canopies (TRAC) instrument, Applied Optics, vol. 31, pp. 7667–7670.

LI-COR, Inc., 1992. LAI-2000 plant canopy analyzer operating manual, LICOR, Inc., Lincoln, Nebr.

McCartney, H.A., 1978. Spectral distribution of solar radiation. I1: Global and diffuse. Quarternary Journal of the Royal Meteorological Society, 104:911-926.

Miller, E.E., Norman, J.M., 1971. A sunfleck theory for plant canopies. I. length of sunlit segments along a transect. Agronomy Journal 63, 735–738.

Miller, J.B., 1967. A formula for average foliage density. Austin Journal of Botanics 15, 141–144.

Nilson, T., Olsson, H., Anniste, J., Lükk, T. and Praks, J. 2001.Thinning-caused change in reflectance of ground vegetation in boreal forest. International Journal of Remote Sensing, 22(14): 2763-2776.

Nilson, T. and Peterson, U. (1991). "A Forest Canopy Reflectance Model and a Test Case". Remote Sensing of Environment, 37:131-142.

Press, W. H.; Flannery, B. P.; Teukolsky, S. A.; and Vetterling, W. T. "Bessel Functions of Fractional Order, Airy Functions, Spherical Bessel Functions." §6.7 in Numerical Recipes in FORTRAN: The Art of Scientific Computing, 2nd ed. Cambridge, England: Cambridge University Press, 1992.

Price, J. C. (1990). On the information content of soil reflectance spectra. Remote Sensing of Environment, 33, 113−121.

Rouse JR., J.W.; Haas, R.H.; Deering, D.W.; Schell, J.A.; Harlan, J.C. (1974): Monitoring the vernal advancement and retrogration (green wave effect) of natural vegetation. Greenbelt: NASA, 1974. 371p. (NASA/GSFC type III final report).

Schlesinger W.H. 1997: Biogeochemistry, an analysis of global change. Academic Press, p. 588.

Spanner,M. A., Pierce, L. L., Peterson, D. L., & Running, S.W. (1990). Remote sensing of temperate coniferous forest leaf area index. The influence of canopy closure, understory vegetation and background reflectance. International Journal of Remote Sensing, 11, 95−111.

Turner, D. P., Cohen, W. B., Kennedy, R. E., Fassnacht, K. S., & Briggs, J. M. (1999). Relationships between leaf area index and Landsat TM spectral vegetation indices across three temperate zone sites. Remote Sensing of Environment, 70, 52−68.

Vermote, E. F., Tanré,D., Deuze, J. L.,Herman, M.,&Morcrette, J. J. (1997). Second simulation of the satellite signal in the solar spectrum, 6S—an overview. IEEE Transactions on Geoscience and Remote Sensing, 35, 675−686.

Welles, J. M., & Norman, J. M. (1991). Instrument for indirect measurement of canopy architecture. Agronomy Journal, 83, 818−825.

11. Appendix

11.1. Appendix 1

11.1.1. Calculation of p_1 and p_2 in FRT

p_1 is calculated as:

$$p_1 = exp(-\tau l_1)\, exp(-\tau l_2)\, C_{HS1}(\alpha) \qquad (X)$$

Where

τ = radiation extinction coefficient (m^{-1}) per unit path length

l_1, l_2 = path lengths within the crown from point M in the directions r_1 and r_2.

C_{HS1} = hot-spot correction factor for α

α = angle between r_1 and r_2

The extinction coefficient, τ, is a function of the leaf area index (LAI (m^2/m^2)), branch area index (BAI (m^2/m^2)) and the crown volume (V).

p_2 is described as:

$$p_2 = a_s(z_1, \theta_1)\, a_s(z_2, \theta_2)\, C_{HS2}(z_1, z_2, l_{12}, r_1, r_2) \qquad (X)$$

Where

$a_s(z, \theta)$ = the average proportion of gaps (free lines of sight) in the canopy at height z in the direction given by the zenith angle θ, assuming bi-nominal distribution of trees.

$C_{HS2}()$ = hot-spot correction factor (taking into account the overlapping of tree crowns)

11.1.2. Calculation of single scattering components in MCRM2

Single scattering of the upper layer is calculated as:

$$\rho_1^{c2} = (\Gamma^{(2)}(r_1, r_2)\, u_L^{(2)} / \mu_1 \mu_2) \int_0^H Q^{(2)}(r1, r2, z)\, dz$$

Where

$\Gamma^{(2)}(r_1, r_2)$ = scattering area phase function of the foliage elements in the upper layer describing the angular distribution of scattering from direction r_1(solar illumination angle) to r_2(veiw angle).

$u_L^{(2)}$ = the leaf area density (m^2/m^3) in the upper layer.

$\mu_i = \cos(r_i)$ where i=1,2.

$Q^{(2)}(r1, r2, z)$ = bi-directional gap probability in the upper layer where z is a height variable.

H = total canopy height.

Single scattering of the lower layer ρ_1^{c1} is calculated according to the same principles as for the upper layer taking into consideration the reducing effects of $Q^{(2)}$ and H on incoming radiation.

$$\rho_1^{c1} = (\Gamma^{(1)}(r_1, r_2)\, u_L^{(1)} / \mu_1 \mu_2)\, Q^{(2)}(r_1, r_2, H) \int_0^{H(1)} Q^{(1)}(r1, r2, z)\, dz$$

Where

$H^{(1)}$ = total height of the lower canopy

The rest of the terms has the same meaning as for the upper layer but are adapted for the lower layer

Single scattering of the soil is calculated as:

$$\rho_1^{soil} = \rho_{soil}(r_1, r_2)\, Q^{(0)}(r_1, r_2, H)$$

Where

$\rho_{soil}(r_1, r_2)$ = soil bi-directional reflectance factor

$Q^{(0)} = Q^{(1)}(r_1, r_2)\, Q^{(2)}(r_1, r_2)$

In bi-directional gap probability terms $Q^{(1)}$ and $Q^{(2)}$ the hot-spot effect is accounted for by using a hot-spot correction factor.

11.2. Appendix 2

A MCRM infile

```
'test 1'                                          : Name of the data set
44.8    0.          .068                          : th0, phi, bAng
2.320   0.2303   1.631                            : L, sl, lmbd_z
11.40   80.76                                     : eln, thm
1000.   0.6998                                    : lmbda, n_ratio
45.     0.4010    0.09166  0.02511  -0.113       : th*, rsli
12.92   0.00965  0.00051  0.00379   0.2774       : cAB, cW, cP, cC, N

*****************************************************************
```

th0, phi, bAng - Sun zenith, view azimuth, and Angstrom turbidity factor
L, sl, lmbd_z - LAI, leaf size parameter and the Markov parameter
eln, thm - LAD parameters
lmbda, n_ratio - Wavelength and a factor for the refractive index
th*, rsli - Soil reflectance parameters
cAB, cW, cP, cC, N - Parameters of the PROSPECT model: chlorophyll content, water content, protein content, cellulose+lignin content, and the leaf structure parameter

11.3. Appendix 3

Table over forest area, main species and important sub-species for all forest stands

stand name	L1	L2	L3	L4	L5
forest area	Skarhult	Skarhult	Fulltofta	Skarhult	Fulltofta
main specie	birch	oak	spruce	oak	beech
sub species	non	beech	non	beech	non

stand name	L6	L7	L8	L9	L10
forest area	Fulltofta	Vomb	Vomb	Vomb	Skarhult
main specie	oak	spruce	spruce	pine	beech
sub species	non	pine, birch	pine	non	non

stand name	L11	L12	L13	L14	L15
forest area	Skarhult	Skarhult	Vomb	Prästaskogen	Prästaskogen
main specie	beech	beech	pine	beech	beech
sub species	non	non	non	non	non

stand name	L16	L17	L18	L19	L20
forest area	Linebjer	Linebjer	Skrylle	Skrylle	Skarhult
main specie	oak	oak	beech	spruce	beech
sub species	hazel	lime, maple, elm	non	non	non

Presentation of the ground cover present in the stands.

L1: Mainly grass with features of small bushes, brackwood, herbs and small groups of ferns. Dead leafs are present to some extent.

L2: Mainly grass, small bushes, herbs and brackwood. Dead leafs is often present.

L3: Mainly dead needles and mosses with features of grass.

L4: Mainly grass, dead leafs and herbs with features of ferns in dense groups and some small bushes.

L5: Mainly herbs, dead leafs and small bushes with features of grass.

L6: Mainly grass, dead leafs and herbs with features of small bushes and brackwood.

L7: Mainly mosses and dead needles with features of dead twigs.

L8: Mainly mosses, grass and herbs with features of needles and dead twigs.

L9: Mainly mosses and grass with features of dead needles and herbs.

L10: Mainly dead leafs with features of small bushes and dead twigs.

L11: Mainly dead leafs and herbs with features of ferns and dead twigs.

L12: Mainly dead leafs with features of dead twigs and small bushes.

L13: Mainly mosses and grass with features of dead needles.

L14: Mainly dead leafs with features of brackwood and some herbs.

L15: Mainly dead leafs with features of herbs and brackwood.

L16: Mainly dead leafs and herbs with features of mosses, ferns, and soil.

L17: Mainly dead leafs with features of herbs and ferns.

L18: Dead leafs.

L19: Mainly mosses, dead needles and dead twigs with features of herbs.

11.4. Appendix 4

FRT infile parameters for a tree main class (infile order)

- Crown form: Always set to ellipsoid (t_ell)
- Stand density (no of trees / m^2): Calculated from stand data.
- Tree height (m): Measured in field.
- Crown length (m): Measured in field.
- Crown radius (m): Measured in field.
- Trunk diameter (cm): Measured in field.
- Total dry leaf weight (kg/tree):
  kg/tree = (LAI_{cl} * SLW_{sp}) / tree density
  where
  LAI_{cl} = % crown area of total crown area (m^2) * stand LAI value (LAI_{Chen})
  (crown area = mean crown area for the measured trees in the size class)
  SLW_{sp} = SLW-value for the given species
- SLW (g / m^2): Calculation procedure given in fieldwork sub-chapter.
- BAI/LAI. BAI: Values measured by Helena Eriksson in year 2003 with Li-Cor. LAI2000 in the leafless period for the deciduous. Spruce values according to Nilson (1999). Pine values according to Rautiainen (2003). LAI: Measured in field by LAI 2000 PCA.
- Tree distribution parameter: Usually set to 1, meaning a slumped tree distribution. Using slightly higher values for stands with regular distribution.
- Shoot shading coefficient: Using tabulated values from the LAI 2000 manual (Li-Cor, 1992) for the given species.
- C1 (chlorophyll content) (% of SLW): Calculated using cAB values given by PROSPECT inversion.
- C2 (water content) (% of SLW): Calculated using EWT values given by PROSPECT inversion.
- C3 (dry matter content) (% of SLW): Calculated using cCL values given by PROSPECT inversion.

- Leaf structural parameter coefficient: Calculated according to formula given in the FRT manual (Kuusk and Nilson, 2002).
- Shoot length (m): Using values in the interval 0.1 – 0.5
- Files of branch and trunk reflectance: Using a spruce trunk reflectance file given with the model.

********** Ground Vegetation **********

- LAI2_ground, upper layer: According to MCRM inversion value.
- sl2_ground (leaf size): According to MCRM inversion value.
- sz2- the Markov parameter: According to MCRM inversion value.
- eln2 (measure of leaf angle distribution): According to MCRM inversion value.
- thm2 - modal leaf angle: According to MCRM inversion value.
- n_ratio2: According to MCRM inversion value.
- SLW2 (g/m^2): According to MCRM inversion value.
- leaf optics model, upper layer: PROSPECT always chosen.
- # of leaf components: 3
- C1 (chlorophyll content, in % of SLW): Calculated from MCRM inversion value.
- C2 (water content in % of SLW): Calculated from MCRM inversion value.
- C3 (dry matter content in % of SLW): Calculated from MCRM inversion value.
- leaf structural parameter coefficient: According to MCRM inversion value.
- LAI1_lower layer: Constant value
- sl1_ground: Constant value
- sz1 (leaf size): Constant value
- eln1 (measure of leaf angle distribution): Constant value
- thm1- modal leaf angle: Constant value
- n_ratio1: Constant value
- SLW1: Constant value
- leaf optics model, lower layer: PROSPECT always chosen.
- # of leaf components: 3
- C1 (chlorophyll content, in % of SLW): Constant value

- C2 (water content) (% of SLW): Constant value
- C3 (dry matter content) (% of SLW): Constant value
- leaf structural parameter coefficient: Constant value

******* soil parameters: Price vectors *******

- s1: According to MCRM inversion value.
- s2: According to MCRM inversion value.
- s3: According to MCRM inversion value.
- s4: According to MCRM inversion value.
- Values for aerosol data (6S): Using values for an atmospheric correction on a Landsat TM scene over Scania recorded 2000-06-10, for details see Eklund et.al. (2003).
- Values for visibility (6S): Using values for an atmospheric correction on a Landsat TM scene over Scania recorded 2000-06-10, for details see Eklund et.al. (2003).
- # sun angles: set to 1. Spectral channels: 200 Spectrum step: 5nm
- Sun zeniths: 44.8
- Spectral channels: 200
- View nadir angle and azimuth angle: Both set to zero in order to simulate Landsat TM image conditions.

11.5. Appendix 5

Important parameters measured and estimated for the forest stands

Stand name	L1	L2	L3	L4	L5	L6	L7
Forest area	Skarhult	Skarhult	Fulltofta	Skarhult	Fulltofta	Fulltofta	Vomb
Species	birch	oak	spruce	oak	beech	oak	spruce
Le (PCA)	2.53	3.12	3.92	2.06	3.04	2.13	3.38
LG	2.53	3.12	5.10	2.06	3.04	2.13	4.39
LC	2.79	2.93	5.78	3.68	2.73	1.78	4.98
Clumping factor	0.72	0.87	0.79	0.46	0.88	0.81	0.79
Stand density(tr/m2)	0.04	0.08	0.05	0.01	0.03	0.02	0.08
Shoot shading	1.00	1.00	1.30	1.00	1.00	1.00	1.30
Tree height (m)	19.90	18.40	25.20	25.10	31.33	18.23	17.60
Trunk diameter (cm)	20.90	26.30	35.86	38.80	57.83	33.20	19.05
Crown radius (m)	1.85	3.04	2.86	3.66	5.17	3.30	2.05
BAI/LAI	0.38	0.24	0.10	0.79	0.28	0.50	0.10
GPS (lat,long) N	6192295	6192463	6200355	6192171	5552615	6200736	6172482
GPS (lat,long) E	1348710	1348647	1364414	1348563	1338960	1364260	1360885

Stand name	L8	L9	L10	L11	L12	L13	L14
Forest area	Vomb	Vomb	Skarhult	Skarhult	Skarhult	Vomb	Prästaskogen
Species	spruce	pine	beech	beech	beech	pine	beech
Le (PCA)	2.72	1.79	3.91	5.31	5.17	2.01	5.08
LG	3.54	3.13	3.91	5.31	5.17	3.52	5.08
LC	4.93	4.43	2.99	5.43	5.21	3.67	5.05
Clumping factor	0.65	0.60	1.00	0.83	0.83	0.82	0.85
Stand density(tr/m2)	0.07	0.03	0.02	0.06	0.06	0.04	0.03
Shoot shading	1.30	1.75	1.00	1.00	1.00	1.75	1.00
Tree height (m)	17.60	21.90	25.50	20.00	18.90	19.70	27.60
Trunk diameter (cm)	19.05	34.60	27.80	29.30	27.80	27.90	44.60
Crown radius (m)	1.46	2.80	4.60	3.66	2.90	2.40	5.10
BAI/LAI	0.10	0.15	0.24	0.22	0.24	0.15	0.21
GPS (lat,long) N	6172247	6173058	6192327	5549981	6191803	6172955	6175323
GPS (lat,long) E	1361121	1360072	1348816	1324236	1349668	1359560	1348636

Stand name	L15	L16	L17	L18	L19
Forest area	Prästaskogen	Linebjer	Linebjer	Skrylle	Skrylle
Species	beech	oak	oak	beech	spruce
Le (PCA)	3.60	4.88	4.65	3.55	3.77
LG	3.60	4.88	4.65	3.55	4.90
LC	3.77	4.13	4.07	3.32	5.76
Clumping factor	0.77	1.00	0.96	0.84	0.77
Stand density(tr/m2)	0.03	0.05	0.05	0.08	0.08
Shoot shading	1.00	1.00	1.00	1.00	1.30
Tree height (m)	32.40	25.20	31.60	17.10	15.50
Trunk diameter (cm)	56.30	84.40	27.90	27.90	24.10
Crown radius (m)	7.10	9.05	6.30	3.55	2.49
BAI/LAI	0.33	0.15	0.17	0.31	0.10
GPS (lat,long) N	6175891	6181093	6180803	6175870	6175096
GPS (lat,long) E	1348208	1342808	1342760	1347076	1347009

11.6. Appendix 6

MCRM parameters used for representing MAX, MIN and MEAN leaf reflectance characteristics in FRT for all the stands

	slw	cAB	cW	cC	N	LAI
L1mv	92.3	37.81	0.01288	0.00923	1.204	1.991
L1max	10	18.55	0.001394	0.001	0.3828	3.541
L1min	10	23.68	0.01565	0.001	0.6324	1.765
L2mv	63.73	26.84	0.01411	0.006373	0.8529	2.853
L2max	10	14.86	0.02764	0.001	0.7126	3.653
L2min	10	43.26	0.001	0.001	1.875	1.028
L3mv	49.33	28.15	0.008663	0.004933	0.895	2.742
L3max	10	14.65	0.001	0.001	0.7083	1.763
L3min	10	1.169	0.001	0.001	0.4984	1.329
L4mv	59.87	14.68	0.001	0.005987	0.4141	2.056
L4max	37.25	16.91	0.001	0.003725	0.8091	4.467
L4min	62.24	15.58	0.001	0.006224	0.8155	0.9564
L5mv	65.2	27.68	0.00113	0.00652	0.905	3.223
L5max	10	33.63	0.002478	0.001	1.174	4.137
L5min	54.57	18.53	0.005502	0.005457	0.4037	2.956
L6mv	63.48	25.92	0.0164	0.006348	0.6895	2.021
L6max	16.33	25.61	0.01672	0.001633	0.8451	2.774
L6min	51.61	9.533	0.01015	0.005161	0.2	1.563
L7mv	51.9	1.645	0.01	0.00519	0.2365	1.363
L7max	93.87	32.1	0.01828	0.009387	0.2	1.648
L7min	10.14	1.815	0.01	0.001014	0.2	1.181
L8mv	57.55	14.28	0.01453	0.005755	0.3515	1.591
L8max	34.84	26.68	0.02694	0.003484	0.7615	1.741
L8min	24.74	0.8804	0.001	0.002474	0.576	0.8947
L9mv	37.1	13.68	0.01185	0.00371	0.2482	2.182
L9max	27.85	9.935	0.001	0.002785	0.2377	3.446
L9min	100	28.73	0.02	0.01	0.3187	1.219
mv10	10	3.867	0.03	0.001	0.3318	0.5
min10	200	1.418	0.0001	0.02	1.371	0.3447
max10	160	7.36	0.001	0.016	1.951	0.5
L11 mv	10	20	0.001	0.001	0.3672	0.3
L11 min	20	10	0.001	0.002	0.5192	0.3
L11max	20	12.17	0.001	0.002	1.931	1
L12mv	30	23.13	0.03	0.003	0.4525	0.5
L12max	77.54	20.78	0.004875	0.007754	0.8205	0.9999
L12min	10	0.001	0.001	0.001	1.5	0.2
L13mv	97.96	20.7	0.001379	0.009796	0.3358	1.94
L13max	165.2	28.31	0.02166	0.01652	0.5452	3.16
L13min	10	36.61	0.03	0.001	0.8277	0.9
L14mv	10	45.7	0.001	0.001	2	0.12
L14max	10	20.75	0.01337	0.001	2	0.7924
L14min	10	0.4937	0.001	0.001	0.1	0.001
L15mv	10	7.474	0.001	0.001	0.2304	0.5
L15max	10	26.45	0.005433	0.001	1.287	1.494
L15min	80	0.001	0.004473	0.008	0.3837	1.148
L16mv	10	20.86	0.001	0.001	0.8486	2.874
L16max	10	7.834	0.01325	0.001	0.3898	2
L16min	10	20	0.001	0.001	0.5092	0.5
L17mv	10	24.46	0.001	0.001	1.336	0.19
L17max	10	13.6	0.001	0.001	1.474	2
L17min	10	0.5178	0.01	0.001	0.2	0.7468
L18mv	10	2.82	0.02	0.001	0.2421	
L18max	10	30	0.001	0.001	0.6417	0.3
L18min	10	20	0.001	0.001	0.6854	0.1
L19mv	69.03	22.5	0.001	0.006903	0.9913	1.696
L19max	206.3	26.27	0.001	0.02063	1.219	1.572

11.7. Appendix 7

Reflectance values and VIs for the Landsat TM sensor calculated from modeled FRT reflectance spectra for MAX, MIN and MV(MAX+MIN/2) for all stands

MV	TM 1 MV	TM 2 MV	TM 3 MV	TM 4 MV	SR MV	NDVI MV	ARVI MV	SAVI MV
L1	0.03481	0.06025	0.03865	0.29315	7.58525	0.76704	0.74683	0.45895
L2	0.02256	0.04434	0.02440	0.27551	11.28918	0.83726	0.82605	0.47087
L3	0.02176	0.04676	0.02375	0.27336	11.50890	0.84011	0.82785	0.46971
L4	0.03014	0.05236	0.04082	0.21353	5.23036	0.67899	0.61130	0.34341
L5	0.03961	0.07885	0.04394	0.31350	7.13525	0.75416	0.73316	0.47157
L6	0.02313	0.04112	0.03108	0.19776	6.36386	0.72840	0.67038	0.34305
L7	0.02553	0.04799	0.02983	0.22590	7.57356	0.76672	0.73749	0.38918
L8	0.02649	0.05017	0.03380	0.21513	6.36552	0.72846	0.67915	0.36318
L9	0.02617	0.05244	0.03119	0.22864	7.33154	0.75995	0.72662	0.38980
L10	0.03993	0.07843	0.05784	0.27165	4.69692	0.64893	0.56392	0.38665
L11	0.04119	0.08344	0.04725	0.29640	6.27268	0.72500	0.69511	0.44298
L12	0.03285	0.06533	0.04208	0.25278	6.00745	0.71459	0.66258	0.39763
L13	0.02186	0.04572	0.02665	0.24934	9.35647	0.80688	0.77609	0.43046
L14	0.02609	0.05075	0.03034	0.26536	8.74616	0.79479	0.76936	0.44304
L15	0.04204	0.08088	0.04987	0.26702	5.35420	0.68525	0.64460	0.39873
L16	0.02599	0.04947	0.02682	0.32996	12.30408	0.84967	0.84541	0.53072
L17	0.02171	0.04478	0.02506	0.29717	11.85930	0.84447	0.82551	0.49641
L18	0.03827	0.07417	0.04542	0.25612	5.63927	0.69876	0.65942	0.39431
L19	0.02442	0.05291	0.02614	0.29713	11.36536	0.83826	0.82848	0.49374
mv	**0.02971**	**0.05790**	**0.03552**	**0.26418**	**7.99923**	**0.76146**	**0.72786**	**0.42707**

MAX	TM 1 MAX	TM 2 MAX	TM 3 MAX	TM 4 MAX	SR MAX	NDVI MAX	ARVI MAX	SAVI MAX
L1	0.03659	0.06453	0.03917	0.36104	9.21748	0.80426	0.79272	0.53633
L2	0.02364	0.04741	0.02467	0.30671	12.43411	0.85113	0.84543	0.50887
L3	0.02073	0.04450	0.02159	0.25854	11.97515	0.84586	0.84023	0.45559
L4	0.02742	0.04938	0.03200	0.23205	7.25225	0.75764	0.72771	0.39275
L5	0.04017	0.08065	0.04426	0.34635	7.82547	0.77338	0.75500	0.50879
L6	0.02210	0.04170	0.02513	0.21655	8.61837	0.79206	0.76993	0.38715
L7	0.02509	0.04604	0.02773	0.22162	7.99304	0.77761	0.75901	0.38812
L8	0.02037	0.04299	0.02378	0.22781	9.58004	0.81096	0.78675	0.40720
L9	0.02676	0.05616	0.03111	0.26141	8.40389	0.78732	0.76116	0.43590
L10	0.04260	0.08344	0.06148	0.29473	4.79355	0.65479	0.57150	0.40862
L11	0.04184	0.08523	0.04712	0.31169	6.61543	0.73738	0.71219	0.46211
L12	0.03118	0.06402	0.03766	0.26691	7.08769	0.75271	0.71622	0.42741
L13	0.02191	0.04614	0.02634	0.27693	10.51497	0.82631	0.80002	0.46795
L14	0.02603	0.05125	0.02858	0.27133	9.49495	0.80943	0.79419	0.45521
L15	0.04281	0.08285	0.04886	0.28570	5.84717	0.70791	0.67759	0.42568
L16	0.02590	0.04949	0.02674	0.33657	12.58679	0.85280	0.84854	0.53833
L17	0.02381	0.04982	0.02463	0.34707	14.08896	0.86745	0.86333	0.55484
L18	0.03795	0.07360	0.04435	0.25194	5.68073	0.70063	0.66468	0.39104
L19	0.02513	0.05472	0.02671	0.33089	12.39031	0.85064	0.84250	0.53204
mv	**0.02958**	**0.05863**	**0.03378**	**0.28452**	**9.07370**	**0.78738**	**0.76467**	**0.45705**

MIN	TM 1 MIN	TM 2 MIN	TM 3 MIN	TM 4 MIN	SR MIN	NDVI MIN	ARVI MIN	SAVI MIN
L1	0.03302	0.05597	0.03813	0.22527	5.90839	0.71050	0.67800	0.36771
L2	0.02148	0.04126	0.02414	0.24430	10.11937	0.82013	0.80228	0.42975
L3	0.02278	0.04902	0.02591	0.28817	11.12046	0.83499	0.81689	0.48323
L4	0.03286	0.05533	0.04965	0.19501	3.92740	0.59411	0.49170	0.29279
L5	0.03904	0.07705	0.04361	0.28065	6.43482	0.73100	0.70693	0.43136
L6	0.02415	0.04055	0.03702	0.17896	4.83379	0.65717	0.56395	0.29736
L7	0.02596	0.04993	0.03193	0.23019	7.20929	0.75637	0.71727	0.39021
L8	0.03260	0.05734	0.04381	0.20244	4.62073	0.64417	0.57258	0.31885
L9	0.02558	0.04871	0.03126	0.19586	6.26461	0.72469	0.68259	0.33955
L10	0.03725	0.07343	0.05419	0.24857	4.58727	0.64204	0.55503	0.36322
L11	0.04055	0.08165	0.04739	0.28112	5.93192	0.71148	0.67656	0.42316
L12	0.03453	0.06665	0.04650	0.23866	5.13257	0.67387	0.60643	0.36711
L13	0.02182	0.04531	0.02696	0.22175	8.22482	0.78319	0.74709	0.39025
L14	0.02615	0.05024	0.03210	0.25938	8.07964	0.77973	0.74411	0.43073
L15	0.04126	0.07890	0.05088	0.24834	4.88079	0.65991	0.60822	0.37059
L16	0.02608	0.04945	0.02689	0.32334	12.02298	0.84643	0.84217	0.52299
L17	0.01961	0.03974	0.02548	0.24726	9.70376	0.81315	0.77495	0.43051
L18	0.03859	0.07474	0.04648	0.26030	5.59971	0.69696	0.65436	0.39753
L19	0.02371	0.05111	0.02558	0.26338	10.29542	0.82294	0.81117	0.45211
mv	**0.02984**	**0.05718**	**0.03726**	**0.24384**	**7.09988**	**0.73173**	**0.68696**	**0.39469**

Lunds Universitets Naturgeografiska institution. Seminarieuppsatser. Uppsatserna finns tillgängliga på Naturgeografiska institutionens bibliotek, Sölvegatan 12, 223 62 LUND. Serien startade 1985.

The reports are available at the Geo-Library, Department of Physical Geography, University of Lund, Sölvegatan 12, S-223 62 Lund, Sweden.
Report series started 1985.

79. Ullman, M., (2001): El Niño Southern Oscillation och dess atmosfäriska fjärrpåverkan.
80. Andersson, A., (2001): The wind climate of northwestern Europe in SWECLIM regional climate scenarios.
81. Lalloo, D., (2001): Geografiska informationssystem för studier av polyaromatiska kolväten (PAH) – Undersökning av djupvariation i BO01-området, Västra hamnen, Malmö, samt utveckling av en matematisk formel för beräkning av PAH-koncentrationer från ett kontinuerligt utsläpp.
82. Almqvist, J., Fergéus, J., (2001): GIS-implementation in Sri Lanka.
Part 1: GIS-applications in Hambantota district Sri Lanka : a case study.
Part 2: GIS in socio-economic planning : a case study.
83. Berntsson, A., (2001): Modellering av reflektans från ett sockerbetsbestånd med hjälp av en strålningsmodell.
84. Umegård, J., (2001): Arctic aerosol and long-range transport.
85. Rosenberg, R., (2002): Tetratermmodellering och regressionsanalyser mellan topografi, tetraterm och tillväxt hos sitkagran och lärk – en studie i norra Island.
86. Håkansson, J., Kjörling, A., (2002): Uppskattning av mängden kol i trädform – en metodstudie.
87. Arvidsson, H., (2002): Coastal parallel sediment transport on the SE Australian inner shelf – A study of barrier morphodynamics.
88. Bemark, M., (2002): Köphultssjöns tillstånd och omgivningens påverkan.
89. Dahlberg, I., (2002): Rödlistade kärlväxter i Göteborgs innerstad – temporal och rumslig analys av rödlistade kärlväxter i Göteborgs artdataarkiv, ADA.
90. Poussart, J-N., (2002): Verification of Soil Carbon Sequestration - Uncertainties of Assessment Methods.
91. Jakubaschk, C., (2002): Acacia senegal, Soil Organic Carbon and Nitrogen Contents: A Study in North Kordofan, Sudan.
92. Lindqvist, S., (2002): Skattning av kväve i gran med hjälp av fjärranalys.
93. Göthe, A., (2002): Översvämningskartering av Vombs ängar.
94. Lööv, A., (2002): Igenväxning av Köphultasjö – bakomliggande orsaker och processer.
95. Axelsson, H., (2003): Sårbarhetskartering av bekämpningsmedels läckage till grundvattnet – Tillämpat på vattenskyddsområdet Ignaberga-Hässleholm.
96. Hedberg, M., Jönsson, L., (2003): Geografiska Informationssystem på Internet – En webbaserad GIS-applikation med kalknings- och försurningsinformation för Kronobergs län.
97. Svensson, J., (2003): Wind Throw Damages on Forests – Frequency and Associated Pressure Patterns 1961-1990 and in a Future Climate Scenario.
98. Stroh, E., (2003): Analys av fiskrättsförhållandena i Stockholms skärgård i relation till känsliga områden samt fysisk störning.

99. Bäckstrand, K., (2004): The dynamics of non-methane hydrocarbons and other trace gas fluxes on a subarctic mire in northern Sweden.
100. Hahn, K., (2004): Termohalin cirkulation i Nordatlanten.
101. Lina Möllerström (2004): Modelling soil temperature & soil water availability in semi-arid Sudan: validation and testing.
102. Setterby, Y., (2004): Igenväxande hagmarkers förekomst och tillstånd i Västra Götaland.
103. Edlundh, L., (2004): Utveckling av en metodik för att med hjälp av lagerföljdsdata och geografiska informationssystem (GIS) modellera och rekonstruera våtmarker i Skåne.
104. Schubert, P., (2004): Cultivation potential in Hambantota district, Sri Lanka
105. Brage, T., (2004): Kvalitetskontroll av servicedatabasen Sisyla
106. Sjöström., M., (2004): Investigating Vegetation Changes in the African Sahel 1982-2002: A Comparative Analysis Using Landsat, MODIS and AVHRR Remote Sensing Data
107. Danilovic, A., Stenqvist, M., (2004): Naturlig föryngring av skog
108. Materia, S., (2004): Forests acting as a carbon source: analysis of two possible causes for Norunda forest site
109. Hinderson, T., (2004): Analysing environmental change in semi-arid areas in Kordofan, Sudan
110. Andersson, J., (2004): Skånska småvatten nu och då - jämförelse mellan 1940, 1980 och 2000-talet
111. Tränk, L., (2005): Kadmium i skånska vattendrag – en metodstudie i föroreningsmodellering.
112. Nilsson, E., Svensson, A.-K., (2005): Agro-Ecological Assessment of Phonxay District, Luang Phrabang Province, Lao PDR. A Minor Field Study.
113. Svensson, S., (2005): Snowcover dynamics and plant phenology extraction using digital camera images and its relation to CO2 fluxes at Stordalen mire, Northern Sweden.
114. Barth, P. von., (2005): Småvatten då och nu. En förändringsstudie av småvatten och deras kväveretentionsförmåga.
115. Areskoug, M., (2005): Planering av dagsutflykter på Island med nätverkanalys
116. Lund, M., (2005): Winter dynamics of the greenhouse gas exchange in a natural bog.
117. Persson, E., (2005): Effect of leaf optical properties on remote sensing of leaf area index in deciduous forest.
118. Mjöfors, K., (2005): How does elevated atmospheric CO2 concentration affect vegetation productivity?
119. Tollebäck, E.,(2005): Modellering av kväveavskiljningen under fyra år i en anlagd våtmark på Lilla Böslid, Halland
120. Isacsson, C., (2005): Empiriska samband mellan fältdata och satellitdata – för olika bokskogområden i södra Sverige.
121. Bergström, D., Malmros, C., (2005): Finding potential sites for small-scale Hydro Power in Uganda: a step to assist the rural electrification by the use of GIS
122. Magnusson, A., (2005): Kartering av skogsskador hos bok och ek i södra Sverige med hjälp av satellitdata.
123. Levallius, J., (2005): Green roofs on municipal buildings in Lund – Modeling potential environmenta benefits.

124. Florén, K., Olsson, M., (2006): Glacifluviala avlagrings- och erosionsformer I sydöstra Skåne – en sedimentologisk och geomorfologisk undersökning.
125. Liljewalch-Fogelmark, K., (2006): Tågbuller i Skåne – befolkningens exponering.
126. Irminger Street, T., (2006): The effects of landscape configuration on species richness and diversity in semi-natural grasslands on Öland – a preliminary study.
127. Karlberg, H., (2006): Vegetationsinventering med rumsligt högupplösande satellitdata – en studie av QuickBirddata för kartläggning av gräsmark och konnektivitet i landskapet.
128 Malmgren, A., (2006): Stormskador. En fjärranalytisk studie av stormen Gudruns skogsskador och dess orsaker.
129 Olofsson, J., (2006): Effects of human land-use on the global carbon cycle during the last 6000 years.
130 Johansson , T., (2006): Uppskattning av nettoprimärproduktionen (NPP) i stormfällen efter stormen Gudrun med hjälp av satellitdata.
131 Eckeskog, M., (2006) Spatial distribution of hydraulic conductivity in the Rio Sucio drainage basin, Nicaragua.
132 Lagerstedt, J., (2006): The effects of managed ruminants grazing on the global carbon cycle and greenhouse gas forcing.